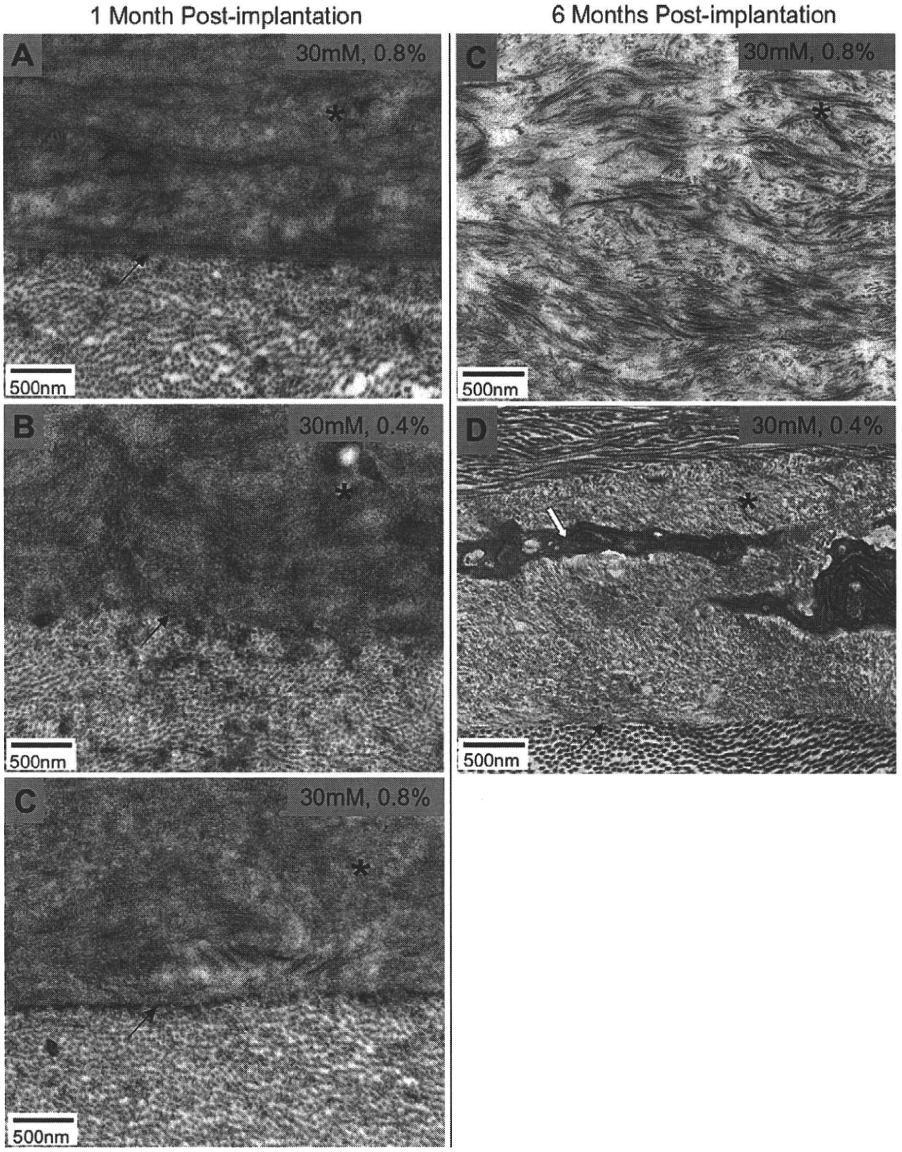

Fig. 8. 1 and 6 months post-implantation. TEM images at ×6000 magnification, of rabbit corneal stroma with various collagen gels implanted into an intra-stromal pocket. Before implantation the gel had a final collagen concentration of 10% (w/w).Asterisks indicates collagen gel implant. Black arrow indicates boundary between host stroma and gel implant. White arrow indicates invading host stromal cell. A: 30 mM NaOH 0.8% EDC/NHS, B: 30 mM NaOH 0.4% EDC/NHS at 1 month post-implantation. C: 30 mM NaOH 0.8% EDC/NHS, D: 30 mM NaOH 0.4% EDC/NHS at 6 months post-implantation.10 mM NaOH, 0.8% EDC/NHS gel was no longer present in the stroma at 6 months post-implantation.

stromal tissue and re-growth of host epithelial cells [32–34,48]. Our findings support the potential use of collagen-based constructs for clinical use as corneal stromal implants. The enhanced stability of the 30 mM NaOH, 0.8% EDC crosslinked gel within the intra-stromal pocket suggests that higher crosslinker levels, when coupled with greater levels of collagen fibrillogenesis, delay the digestion or degradation of the construct. However, the detrimental effect that these levels have on transparency of the gel must be taken into consideration. In addition, oedma in the anterior stroma suggests that the most stable gel (30 mM of NaOH, 0.8% EDC/NHS) may act as a barrier, preventing the endothelial pump from properly regulating anterior stromal hydration.

5. Conclusions

It is clear that within our constructs the assembly of type I collagen molecules can be manipulated over a wide pH range. In addition, even minor changes in the environmental conditions of the gels (such as pH), dramatically affects the optical and mechanical properties of the constructs. It was therefore necessary to establish a balance between the solution pH and crosslinker concentration. Nevertheless, whilst *in vitro* analysis can highlight the fundamental processes that govern fibrillogenesis, we must be careful to observe the limitations of any comparisons made to natural collagen assembly, as the complex arrangement of keratocytes and ECM macromolecules creates a unique and influential environment that cannot currently be replicated *in vitro. In vivo* implantation of the hydrogels into intra-stromal pockets demonstrated favourable biocompatibility, and highlighted the effect of higher levels of both fibrillogenesis and crosslinking on increased long term survival of the gels. Further work will be aimed at enhancing the optical and mechanical properties of the gels, and improving their long term *in vivo* characteristics through the addition of other ECM molecules. Presently, the optically transparent crosslinked collagen gels used in this study provide a basis for the future production of more complex biomimetic stromal

constructs utilizing orthogonally stacked layers of aligned collagen. The gels used in this study have potential clinical use as drug carriers, as protective membranes for corneal surface damage, and stromal implantation for tissue replacement and regeneration.

Acknowledgements

We thank EPSRC (UK) and Global COE (Japan) for supporting this study. This work was supported in part by grants from the United Kingdom Engineering and Physical Sciences Research Council (Grant no. EP/F034970/1 to AJQ), the Grants-in-Aid for Scientific Research from the Ministry of Health Labor and Welfare, and from the Ministry of Education, Culture, Sports, Science, and Technology in Japan, and by the Tohoku University Global COE for conquest of Signal Transduction Disease with "Network Medicine". The authors confirm that there are no known conflicts of interest associated with this publication and there has been no significant financial support for this work that could have influenced its outcome.

References

[1] Meek KM, Leonard DW. Ultrastructure of the corneal stroma: a comparative study. Biophys J 1993;64:273–80.
[2] Quantock AJ, Meek KM, Fullwood NJ, Zabel RW. Scheie's syndrome: the architecture of corneal collagen and distribution of corneal proteoglycans. Can J Ophthalmol 1993;28:266–72.
[3] Hogan MJ, Alvarado JA, Weddel JE. Histology of the Human Eye. Philadelphia: WB Saunders; 1971. pp. 55–111, 183–201.
[4] Komai Y, Ushiki T. The three-dimensional organization of collagen fibrils in the human cornea and sclera. Invest Ophthalmol Vis Sci 1991;32:2244–58.
[5] Ivarsen A, Fledelius W, Hjortdal JO. Three-year changes in epithelial and stromal thickness after PRK or LASIK for high myopia. Invest Ophthalmol Vis Sci 2009;50:2061–6.
[6] Hayashida Y, Akama TO, Beecher N, Lewis P, Young RD, Meek KM, et al. Matrix morphogenesis in cornea is mediated by the modification of keratan sulfate by GlcNAc 6-O-sulfotransferase. Proc Natl Acad Sci U S A 2006;103:13333–8.
[7] Henriksson JT, McDermott AM, Bergmanson JPG. Dimensions and morphology of the cornea in three strains of mice. Invest Ophthalmol Vis Sci 2009;50:3648–54.
[8] Müller L, Pels E, Vrensen G. The specific architecture of the anterior stroma accounts for maintenance of corneal curvature. Br J Ophthalmol 2001;85:437–43.
[9] Quantock AJ, Young RD, Tomoya AO. Structural and biochemical aspects of keratan sulphate in the cornea. Cell Mol Life Sci 2010;67:891–906.
[10] Maurice DM. The structure and transparency of the corneal stroma. J Physiol 1957;136:263–86.
[11] Hart RW, Farrell RA. Light scattering in the cornea. J Opt Soc Am 1969;59:766–74.
[12] Benedek GB. Theory and transparency of the eye. Appl Opt 1971;10:459–73.
[13] Birk DE, Fitch JF, Babiarz JP, Doane KJ, Linsenmayer TF. Collagen fibrillogenesis in vitro: interaction of types I and V collagen regulates fibril diameter. J Cell Sci 1990;95:649–57.
[14] Zhang G, Chen S, Goldoni S, Calder BW, Simpson HC, Owens RT, et al. Genetic evidence for the coordinated regulation of collagen fibrillogenesis in the cornea by decorin and biglycan. J Biol Chem 2009;284:8888–97.
[15] Lewis PN, Pinali C, Young RD, Meek KM, Quantock AJ, Knupp C. Structural interactions between collagen and proteoglycans are elucidated by three-dimensional electron tomography of bovine cornea. Structure 2010;18:239–45.
[16] Meek KM, Boote C. The use of X-ray scattering techniques to quantify the orientation and distribution of collagen in the corneal stroma. Prog Retin Eye Res 2009;28(5):369–92.
[17] Jester JV, Møller-Pedersen T, Huang J, Sax CM, Kays WT, Cavangh HD, et al. The cellular basis of corneal transparency: evidence for 'corneal crystallins'. J Cell Sci 1999;112:613–22.
[18] Jester JV. Corneal crystallins and the development of cellular transparency. Semin Cell Dev Biol 2008;19:82–93.
[19] Hu X, Lui W, Cui L, Wang M, Cao Y. Tissue engineering of nearly transparent corneal stroma. Tissue Eng 2005;11(11–12):1710–7.
[20] Orwin EJ, Borene ML, Hubel A. Biomechanical and optical characteristics of a corneal stromal equivalent. J Biomech Eng 2003;125:439–44.
[21] Ruberti JW, Zieske JD. Prelude to corneal tissue engineering – gaining control of collagen organization. Prog Retin Eye Res 2008;27(5):549–77.
[22] Germain L, Auger FA, Grandbois E, Guignard R, Giasson M, Boisjoly H, et al. Reconstructed human cornea produced in vitro by tissue engineering. Pathobiology 1999;67(3):140–7. LOEX.
[23] Griffith M, Hakim M, Shimmura S, Watsky M, Li F, Carlsson D, et al. Artificial human corneas: scaffolds for transplantation and host regeneration. Cornea 2002;2l(Suppl. 2):S54–61.
[24] Schneider AI, Maier-Reif K, Graeve T. Constructing an in vitro cornea from cultures of the three specific corneal cell types. In Vitro Cell Dev Biol Anim 1999;35(9):515–26.
[25] Tegtmeyer S, Papantoniou I, Muller-Goymann CC. Reconstruction of an in vitro cornea and its use for drug permeation studies from different formulations containing pilocarpine hydrochloride. Eur J Pharm Sci 2001;51 (2):119–25.
[26] Chen CS, Yannas IV, Spector M. Pore strain behaviour of collagen-glycosaminoglycan analogues of extracellular matrix. Biomaterials 1995;16 (10):777–83.
[27] Matsuda K, Suzuki S, Isshiki N, Yoshioka K, Okada T, Ikada Y. Influence of glycosaminoglycans on the collagen sponge component of a bilayer artificial skin. Biomaterials 1990;11(5):351–5.
[28] Osborne CS, Barbenel JC, Smith D, Savakis M, Grant MH. Investigation into the tensile properties of collagen/chondroitin-6-sulphate gels: the effect of crosslinking agents and diamines. Med Biol Eng Comput 1998;36(1):129–34.
[29] Yannas IV, Burke JF. Design of an artificial skin. I. Basic design principles. J Biomed Mater Res 1980;14(1):65–81.
[30] Tanaka Y, Kubota A, Matsusaki M, Duncan T, Hatakeyama Y, Fukuyama K, et al. Anisotropic mechanical properties in collagen hydrogels induced by uniaxial-flow for ocular applications. J Biomater Sci Polym Ed; 2010, [Epub ahead of print].
[31] Rafat M, Li F, Fagerholm P, Lagali NS, Watsky MA, Munger R, et al. PEG-stabilized carbodiimide crosslinked collagen–chitosan hydrogels for corneal tissue engineering. Biomaterials 2008;29(29):3960–72.
[32] Liu Y, Gan L, Carlsson DJ, Fagerholm P, Lagali N, Watsky MA, et al. A simple, crosslinked collagen tissue substitute for corneal implantation. Invest Ophthalmol Vis Sci 2006;47(5):1869–75.
[33] Liu Y, Griffith M, Watsky MA, Forrester JV, Kuffova L, Grant D, et al. Properties of porcine and recombinant human collagen matrices for optically clear tissue engineering applications. Biomacromolecules 2006;7(6):1819–28.
[34] Liu W, Merrett K, Griffiths M, Fagerholm P, Dravida S, Heyne B, et al. Recombinant human collagen for tissue engineered corneal substitutes. Biomaterials 2008;29(9):1147–58.
[35] Bard JB, Chapman JA. Polymorphism in collagen fibrils precipitated at low pH. Nature 1968;219:1279–80.
[36] Leibovich SJ, Weiss JB. Electron microscope studies of the effects of endo- and exopeptidase digestion on tropocollagen. A novel concept of the role of terminal regions in fibrillogenesis. Biochim Biophys Acta 1970;214 (3):445–54.
[37] Zeng Y, Yang J, Huang K, Lee Z, Lee X. A comparison of biomechanical properties between human and porcine cornea. J Biomech 2001;34(4):533–7.
[38] Crabb RA, Chau EP, Evans MC, Barocas VH, Hubel A. Biomechanical and microstructural characteristics of a collagen film-based corneal stroma equivalent. Tissue Eng 2006;12(6):1565–75.
[39] Christiansen DL, Huang EK, Frederick HS. Assembly of type I collagen: fusion of fibril subunits and the influence of fibril diameter on mechanical properties. Matrix Biol 2000;19(5):409–20.
[40] Roeder BA, Kokini K, Sturgis JE, Robinson JP, Voytik-Harbin SL. Tensile mechanical properties of three-dimensional type I collagen extracellular matrices with varied microstructure. J Biomech Eng 2002;124:214–22.
[41] Parry DA. The molecular and fibrillar structure of collagen and its relationship to the mechanical properties of connective tissue. Biophys Chem 1988;29 (1–2):195–209.
[42] Trelstad RL, Hayashi K, Gross J. Collagen fibrillogenesis: intermediate aggregates and suprafibrillar order. Proc Natl Acad Sci U S A 1976;73(11):4027–31.
[43] Watson PG, Young RD. Scleral structure, organisation and disease. A review. Exp Eye Res 2004;78(3):609–23.
[44] Harris JR, Reiber A. Influence of saline and pH on collagen type I fibrillogenesis in vitro: fibril polymorphism and colloidal gold labelling. Micron 2007;38 (5):513–21.
[45] Cisneros DA, Hung C, Franz CM, Muller DJ. Observing growth steps of collagen self-assembly by time-lapse high-resolution atomic force microscopy. J Struct Biol 2006;154(3):232–45.
[46] Gelman RA, Poppke DC, Piez KA. Collagen fibril formation in vitro. The role of the nonhelical terminal regions. J Biol Chem 1979;254(22):11741–5.
[47] Graham HK, Holmes DF, Watson RB, Kadler KE. Identification of collagen fibril fusion during vertebrate tendon morphogenesis. The process relies on unipolar fibrils and is regulated by collagen-proteoglycan interaction. J Mol Biol 2000;295(4):891–902.
[48] Merrett K, Liu W, Mitra D, Camm KD, McLaughlin CR, Liu Y, et al. Synthetic neoglycopolymer-recombinant human collagen hybrids as biomimetic crosslinking agents in corneal tissue engineering. Biomaterials 2009;30 (29):5403–8.

Graefes Arch Clin Exp Ophthalmol
DOI 10.1007/s00417-010-1566-8

RETINAL DISORDERS

Safety threshold of intravitreal activated protein-C

Kentaro Nishida · Motohiro Kamei · Zhao-jiang Du · Ping Xie · Takuhiro Yamamoto · Mihoko Suzuki · Hirokazu Sakaguchi · Kohji Nishida

Received: 10 August 2010 / Revised: 6 October 2010 / Accepted: 29 October 2010

Abstract
Purpose Although activated protein C (APC) is effective in preventing the death of retinal neurons in ischemic retinopathy, it is not known at what concentrations it becomes retinotoxic. The purpose of this study was to determine the concentrations of intravitreal APC that are safe and those that are toxic for the retina, using rabbit eyes.
Methods The left eyes of 12 rabbits received an intravitreal injection of 1.5 to 150 μg of APC in 0.1 ml of saline. The fellow eyes were treated with an intravitreal injection of the same amount of saline. Slit-lamp examination, fundus examination, fluorescein angiography (FA), and electroretinograms (ERGs) were performed before and at different times after the injection. The eyes were enucleated at 6 months after the injection and examined histologically.
Results The clinical and histological differences between the control eyes and the eyes that had APC injections up to 15 μg were not significant. Localized retinal edema was observed in two of three eyes with 150 μg of APC immediately after the injection. In these two eyes, chorioretinal atrophy was observed in the area of the retinal edema at 6 months, which corresponded with a hyperfluorescent area in the FA images and focal retinal degeneration histologically. No significant changes were detected in the full-field ERGs in the eyes treated even with 150 μg of APC throughout the observation period.
Conclusion Our results show that an intravitreal injection of APC at a dose ≤15 μg is safe, but 150 μg of APC can be toxic to the retina.

Keywords Activated protein C (APC) · Safety · Toxicity · Retina · Intravitreal injection

K. Nishida · M. Kamei (✉) · Z.-j. Du · P. Xie · T. Yamamoto · M. Suzuki · H. Sakaguchi · K. Nishida
Department of Ophthalmology,
Osaka University Graduate School of Medicine,
2-2 Yamadaoka, #E7,
Suita 565-0871, Japan
e-mail: mkamei@ophthal.med.osaka-u.ac.jp

Introduction

Retinal ischemia can lead to blindness, and is the underlying mechanism of a number of sight-threatening disorders including central retinal artery occlusion, ischemic central retinal vein thrombosis, diabetic retinopathy, and some types of glaucoma [1, 2]. Activated protein C (APC) is a serine protease with anticoagulant and anti-inflammatory activities. APC has recently been described as a promising drug for ischemic stroke due to its cytoprotective and antiapoptotic activities in many clinical observations, in vitro studies, and animal models of focal ischemic injuries [3–7]. These findings increase the possibility that APC can be used to treat retinal ischemic diseases. We have shown the efficacy of an intravitreal injection of APC in a retinal ischemic model [8].

The results of our recent study showed that an intravitreal injection of 0.06 μg of APC has a neuroprotective effect on retinal neurons in a central retinal vein occlusion (CRVO) rat model [8]. However, before APC is used for retinal ischemic diseases, evidence must be obtained that it is not toxic to ocular tissues. Unfortunately, toxicological profiles of APC on ocular tissues have not been published.

Thus, the purpose of this study was to determine the concentrations of intravitreal APC that are safe and those that are toxic for rabbit eyes.

Published online: 24 November 2010

Materials and methods

Animals

Twelve Dutch-belted rabbits (Biotech, Saga, Japan) weighing between 1.8 kg and 2.2 kg were studied. All procedures conformed to the ARVO Statement for the Use of Animals in Ophthalmic and Vision Research. Animals with corneal or lens opacities or retinal damage before the study were excluded.

Intravitreal injection

The intravitreal injection of APC (Anact C®; Kaketsuken, Kumamoto, Japan) was performed after the baseline examinations. The rabbits were anesthetized by an intramuscular injection of ketamine hydrochloride (33 mg/kg) and xylazine hydrochloride (8.5 mg/kg), and the pupils were dilated with 0.5% tropicamide and 0.5% phenylephrine hydrochloride. Then 1.5 μg to 150 μg of APC was injected into the vitreous in a volume of 0.1 ml saline with a 27-gauge needle. The needle was inserted 1.5 mm posterior to the superotemporal limbus while the eye was viewed under an operating microscope. To prevent a reflux of APC, the needle was held in place for 10 seconds and a paracentesis of the anterior chamber was performed. Eye drops of 0.3% levofloxacin (Cravit®; Santen, Osaka, Japan) was applied to the eyes immediately after the injection.

The left eye of each animal was injected intravitreally with 1.5 μg, 15 μg, and 150 μg APC/0.1 ml saline. There were four eyes that received 1.5 μg APC/0.1 ml saline (group 1), four eyes with 15 μg APC/0.1 ml saline (group 2), and four eyes with 150 μg APC/0.1 ml saline (group 3). The estimated concentrations of APC in the eyes were approximately 1 μg/ml in group 1, 10 μg/ml in group 2, and 100 μg/ml in group 3, assuming a 1.5 ml of vitreous [9]. The contralateral right eye of each animal received an intravitreal injection of an equivalent amount of vehicle solution (saline solution).

Clinical examinations

Baseline examinations were performed by slit-lamp biomicroscopy, indirect ophthalmoscopy, and fluorescein angiography (FA). The condition of the conjunctiva, cornea, anterior chamber, crystalline lens, vitreous, retina, and choroid were evaluated for the presence of inflammation, opacities, hemorrhages, and complications. All of the fundi were photographed with a fundus camera (TRC-50IX; TOPCON, Tokyo, Japan). Slit-lamp examinations, fundus examinations, and electroretinograms were done at 3 days, 1 week, 1 month, 3 months, and 6 months after the injection. The fundus photographs and FA images were examined before and 6 months after the treatment.

Electroretinograms

Electroretinograms (ERGs) were recorded with an ERG system equipped with a contact lens electrode (8017BFPW-4 ERG electrode, Mayo, Nagoya, Japan) and an electronic pulse generator (LS-704B, SLS-3100; Nihon Kohden, Tokyo, Japan). The rabbits were anesthetized with an intramuscular injection of 40 mg/kg ketamine and 4 mg/kg xylazine, and the corneas were topically anesthetized. Topical hydroxypropyl methylcellulose (2.5%) was used to electrically connect the cornea to the electrodes in the contact lens. ERGs were recorded after dark-adaption for 20 min. The flash stimuli were obtained from a stroboscopic unit (LS-704B: Nihon Kohden) which was controlled by the electronic pulse generator (SLS-3100: Nihon Kohden). The strobe flash unit was placed 15 cm in front of the rabbit's eye; the energy of the light was set at 1.2 J, and the stimulus duration was 32 μs.

The a-wave amplitude was measured from the baseline to the first negative trough, and the b-wave from the negative trough to the positive peak. Ten ERGs with a stimulus interval of 5 seconds were averaged by a computer (Neuropack μ. Model MEB-9104; Nihon Koden). The amplitudes and implicit times of the a- and b-waves of the injected eyes were compared to that at the baseline.

Histological examinations

After the final examination at 6 months, the rabbits were euthanized with a 5-ml intravenous injection of pentobarbital (50 mg/ml). The eyes were enucleated, fixed in 4% paraformaldehyde and 2.5% glutaraldehyde, dissected, and embedded in paraffin. Paraffin sections of 4 μm thickness were cut and stained with hematoxylin and eosin. The sections were examined under a light microscope and photographed with a CCD camera (AxioCam, Carl Zeiss Japan, Tokyo, Japan). The images were analyzed with Axio Vision 2.0 (Carl Zeiss Japan) software. Three sections perpendicular to and at the center of the visual streak were analyzed. In addition, sections 5 mm on either side of the center of the visual streak were also analyzed.

Statistical analyses

Statistical analyses were performed with the SigmaStat (ver.2.0; SYSTAT, San Jose, CA, USA). One-way ANOVA was used to determine the significance of the differences in the ERGs between the three groups at each selected time point and baseline. One-way repeated measures ANOVA was used to calculate the significance of the differences in the ERGs between each selected time point and baseline. A value of $P<0.05$ was considered statistically significant.

Results

Clinical examinations

Slit-lamp biomicroscopy and ophthalmoscopy were used to detect clinical signs of toxicity. No inflammation was observed in either the experimental or control eyes. The ocular media were clear except for a mild cataract in one eye of group 1 and one eye of the control group. The retina and optic nerve appeared unaltered in group 1 and group 2. Because of one rabbit death in group 3 from the anesthesia during the follow-up examinations, we excluded the rabbit from this analysis. Localized retinal edema was seen in two of three eyes in group 3 immediately after the injection of APC, and focal chorioretinal atrophy (approximately 6.2 disc areas on an average) was observed in the area of the retinal edema at 6 months. A hyperfluorescent area was detected by FA at the area of the edema (Fig. 1).

Electroretinograms

The a- and b-waves of the ERGs in the APC-injected eyes at 6 months after the injection were not significantly different from those recorded before the injection (Fig. 2; $P>0.05$; Fig. 3). There were no significant differences in the ERGs between the three groups at any times ($P>0.05$, Fig. 3). We did not observe functional changes on the whole in any group from the ERGs. Although focal functions may be deteriorated in the area of localized edema, no functional change was detected by the full field ERGs.

Histological findings

There were no differences in the histological appearances between the APC-injected eyes and vehicle-injected eyes in group 1 and group 2 (Fig. 4). However, two of three of the APC-treated eyes in group 3 had localized morphologic

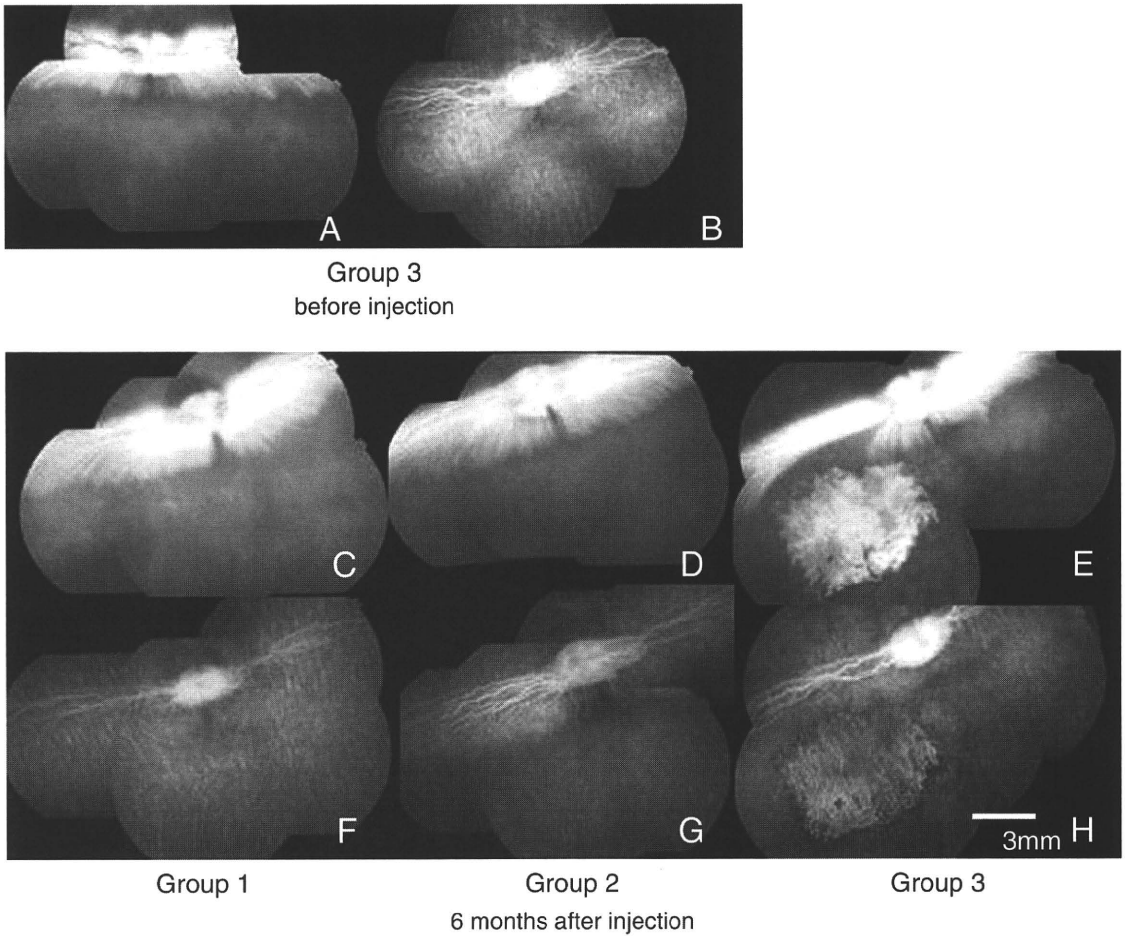

Fig. 1 Representative fundus photographs (**a**, **c-e**) and fluorescein angiograms (**b**, **f-h**) of experimental eyes in group 3 before APC injection and in each group at 6 months after the APC injection. There is no significant change in group 3 before APC injection (**a**, **b**), but at 6 months after APC injection well-defined chorioretinal atrophy can be seen in an eye from group 3 (**e**). The atrophy is seen as a hyperfluorescent area in the FA (**h**). There are no changes in groups 1and 2 (**c**, **d**, **f**, and **g**) at 6 months after the APC injection

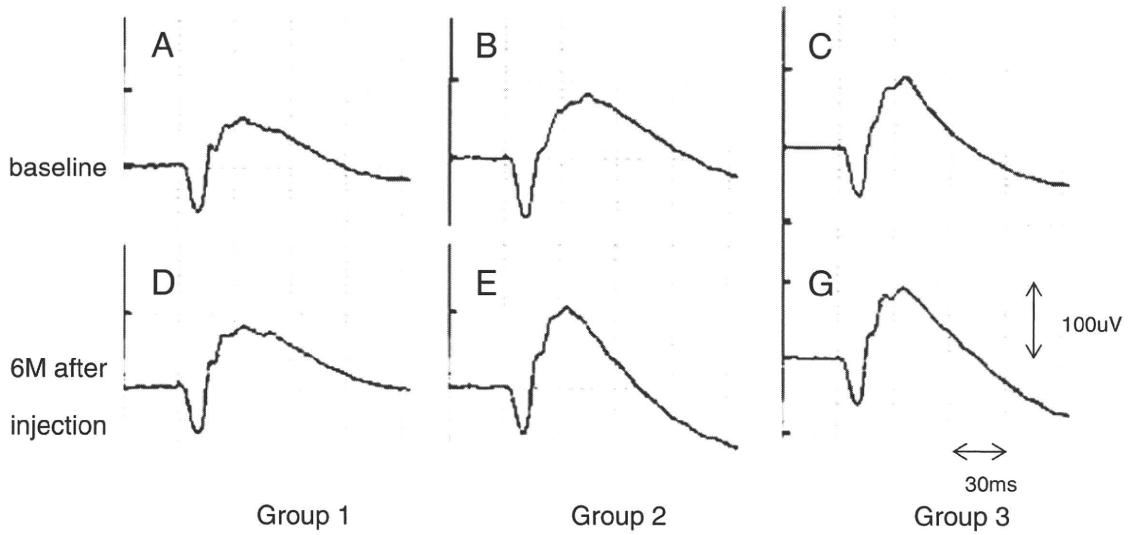

Fig. 2 Representative ERGs of experimental eyes in groups 1, 2, and 3 at baseline (**a**, **b** and **c**) and 6 months after APC injection (**d**, **e** and **g**)

retinal damage, including damaged retinal structures and decreased thickness of the retinal layers (Fig. 4e and j). No pathologic changes were observed outside the damaged retinal area, which corresponded to the area of retinal edema detected by indirect ophthalmoscopy immediately after injection and choroiretinal atrophy detected by FA at 6 months.

Discussion

Previous experimental studies have shown that an intravitreal injection of APC may have neuroprotective effects against ischemic neuronal diseases because of APC's cytoprotective and anti-apoptotic activities [3–7]. We

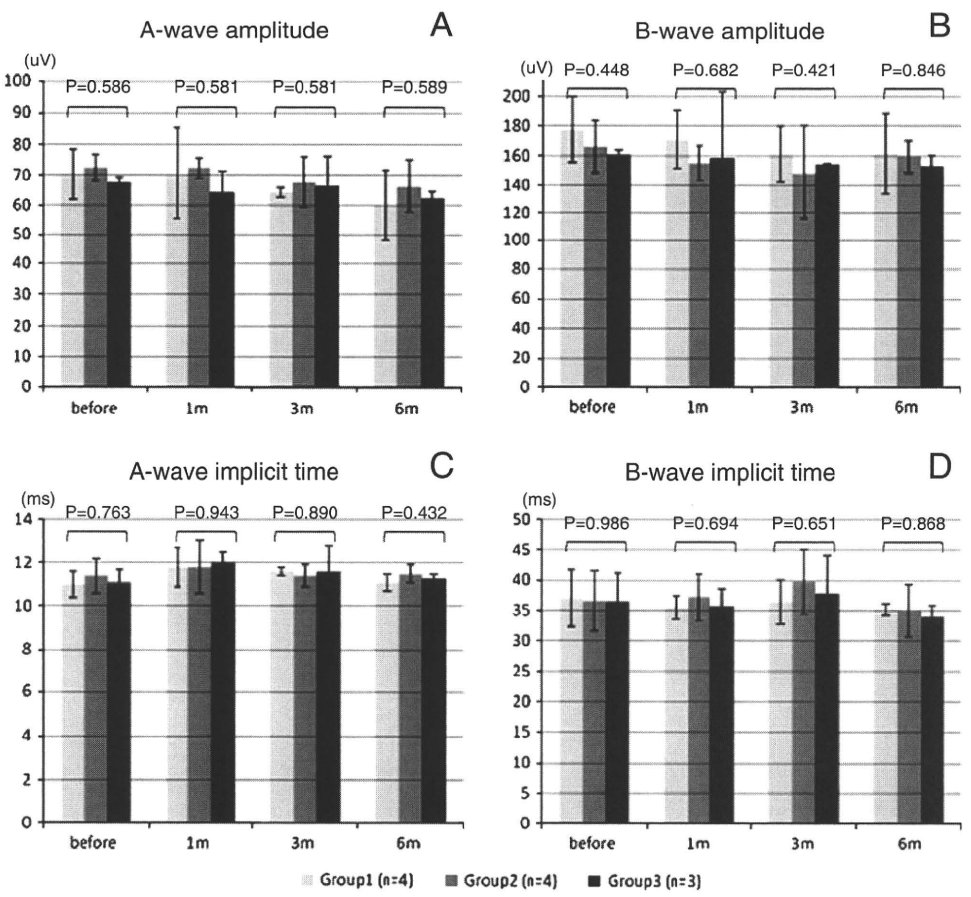

Fig. 3 Follow-up ERGs after APC injection in the three groups of eyes that were injected with 1.5 μg (group 1), 15 μg (group 2), or 150 μg (group 3) APC. Amplitude of a-wave (**a**) and b-wave (**b**), and implicit times of a-wave (**c**) and b-wave (**d**). There are no significant differences in the ERG parameters between the three groups at any time ($P>0.05$, one-way ANOVA)

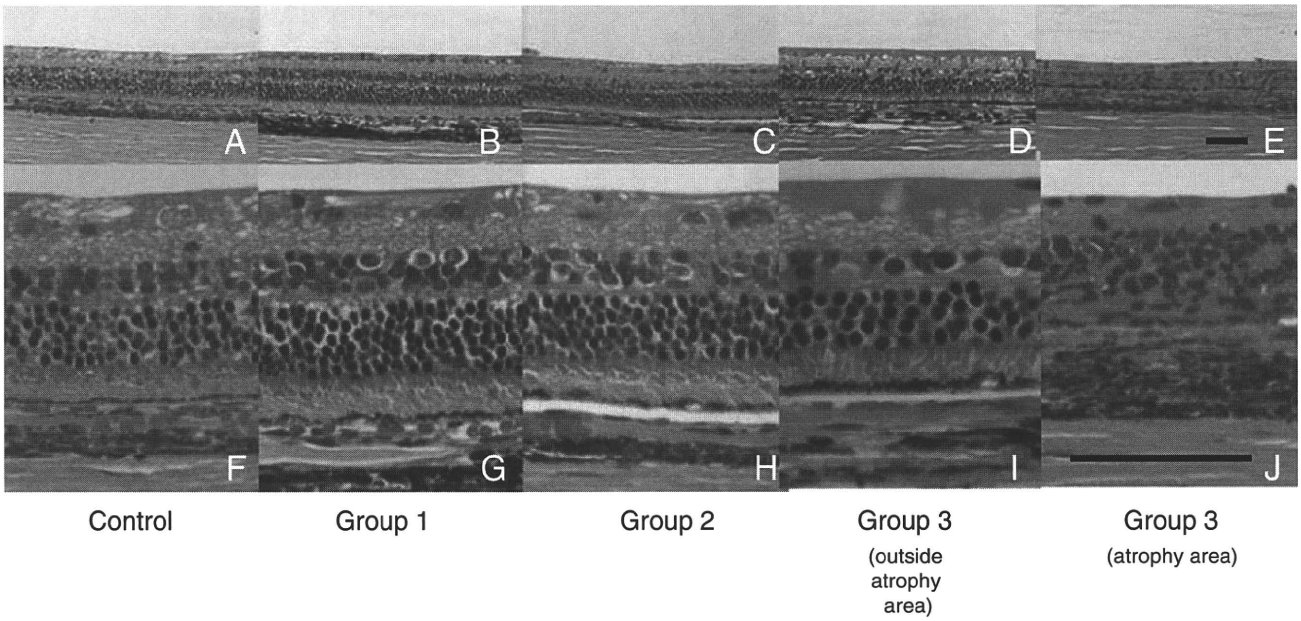

Fig. 4 Histopathology of a control eye (**a, f**) and experimental eyes in group 1 (**b, g**), group 2 (**c, h**) and group 3 (**d, e, i** and **j**). Sections (**a-c, e-h** and **j**) were made 5 mm away from the center of the visual streak where the chorioretinal atrophy was observed in group 3. Section (**d** and **i**) was made 2 mm away from the chorioretinal atrophy. In the atrophy area in group 3 (**e, j**) all retinal layers are damaged and the retina is thinner than the control eye (**a, f**). But the eyes in group 1 (**b** and **g**) and group 2 (**c** and **h**) do not show any histological changes. No histological changes can be seen in the area away from the atrophic area in group 3 (**d** and **i**). Scale, 50 μm

recently demonstrated that APC protected retinal neurons under ischemic conditions [8]. In this study, we determined the safety threshold of APC before its clinical application. Our results demonstrated that 1.5 μg and 15 μg of intravitreal APC injection were safe for rabbit eyes, and that 150 μg may be a toxic level. This is consistent with the results of our earlier in vitro experiment [8], that APC in high doses is cytotoxic to cultured retinal cells. We speculate the following molecular mechanisms for the toxicity of high dose APC; calcium influx, NFκ-B down regulation, or inhibition of NO synthesis. An experiment on human brain endothelial cells showed that APC increased the intracellular calcium concentration [10], and another experiment demonstrated a decrease of NFκ-B in rat hippocampal neurons [11]. There is also another report that APC blocks NO synthesis in rats [12]. These changes in signal transduction may be exaggerated with high doses of APC and may cause retinal edema. The reason why the toxic change appeared in a localized area is suggested by the explanation in a study of gentamicin retinal toxicity [13, 14], which emphasized the importance of needle-tip location and rapidity of injection during intravitreal injection. If the tip was close to the retina or if the injection was given rapidly, a sharply demarcated area of retinal edema, which is similar to the change observed in the current study, was observed and eventually developed extensive changes in the retina and RPE. The reason why not all of the eyes in group 3 had retinal changes, therefore, might be the difference of needle-tip location and rate of injection during the intravitreal injection.

Although we conclude that the threshold dose for safety of APC is between 15 and 150 μg, our ERG data demonstrated no significant changes in the full-field a- and b-waves in all experimental eyes, even in group 3 (150 μg of APC). The full-field ERG evaluation was not sensitive enough to detect localized retinal damage observed in group 3. Neverthless, our results showed that intravitreal injection of APC, even at the highest dose (150 μg), did not impact the entire retinal function.

Although our results provide some clues to the clinical safety of APC in ischemic retinal diseases, rabbit eyes differ from human eyes in vitreous volume and retinal vascular anatomy. Moreover, we used the normal rabbit for this experiment; this should be considered when extrapolating our studies to safety in human subjects.

Intravitreal injections are common procedures, with a relatively low incidence of complications when used to treat vitreoretinal diseases [15–19]. Our results show that intravitreal injection of APC with a dose lower than 15 μg (10 μg/ml) can be safe in rabbit normal eyes. A total dose of 0.06 to 0.6 μg of APC in rat eyes (approximately 3 μg/ml) is effective in protecting the retina from ischemia. These findings indicate that the concentration of APC which is high enough to protect the retina from ischemic conditions is lower than the safety threshold.

References

1. Campochiaro PA (2000) Retinal and choroidal neovascularization. J Cell Physiol 184:301–310
2. Kaur C, Foulds WS, Ling EA (2008) Hypoxia–ischemia and retinal ganglion cell damage. Clin Ophthalmol 2:879–889
3. Fernández JA, Xu X, Liu D, Zlokovic BV, Griffin JH (2003) Recombinant murine-activated protein C is neuroprotective in a murine ischemic stroke model. Blood Cells Mol Dis 30:271–276
4. Guo H, Liu D, Gelbard H, Cheng T, Insalaco R, Fernandez JA, Griffin JH, Zlokovic BV (2004) Activated protein C prevents neuronal apoptosis via protease activated receptors 1 and 3. Neuron 41:563–572
5. Liu D, Cheng T, Guo H, Fernandez JA, Griffin JH, Song X, Zlokovic BV (2004) Tissue plasminogen activator neurovascular toxicity is controlled by activated protein C. Nat Med 10:1379–1383
6. Zlokovic BV, Zhang C, Liu D, Fernandez JA, Griffin JH, Chopp M (2005) Functional recovery after embolic stroke in rodents by activated protein C. Ann Neurol 58:474–477
7. Weiler H, Ruf W (2008) Activated protein C in sepsis: the promise of nonanticoagulant activated protein C. Curr Opin Hematol 15:487–493
8. Du Z, Yamamoto T, Ueda T, Suzuki M, Tano Y, Kamei M (2010) Activated protein C rescues the retina from ischemia-induced cell death. Invest Ophthalmol Vis Sci, doi:10.1167/iovs.10-5557
9. Morrison VL, Koh HJ, Cheng L, Bessho K, Davidson MC, Freeman WR (2006) Intravitreal toxicity of the kenalog vehicle (benzyl alcohol) in rabbits. Retina 26:339–344
10. Domotor E, Benzakour O, Griffin JH, Yule D, Fukudome K, Zlokovic BV (2003) Activated protein C alters cytosolic calcium flux in human brain endotherium via binding to endotherial protein C receptor and activation of protease activated receptor-1. Blood 101:4797–4801
11. Gorbacheva L, Pinelis V, Ishiwata S, Strukova S, Reiser G (2010) Activated protein C prevents glutamate-and thrombin-induced activation of nuclear factor-kappaB in cultured hippocamapal neurons. Neuroscience 165:1138–1146
12. Gupta A, Berg DT, Gerlitz B, Richardson MA, Galbreath E, Syed S, Sharma AC, Lowry SF, Grinnell BW (2007) Activated protein C suppresses adrenomedullin and ameliorate lipopolysaccharifde-induced hypotension. Shock 28:468–476
13. Zachary IG, Forster RK (1976) Experimental intravitreal gentamicin. Am J Ophthalmol 82:604–611
14. McDonald HR, Schatz H, Allen AW, Chenoweth RG, Cohen HB, Crawford JB, Klein R, May DR, Snider JD 3rd (1986) Retinal toxicity secondary to intraocular gentamicin injection. Ophthalmology 93:871–877
15. Rosenfeld PJ, Schwartz SD, Blumenkranz MS, Miller JW, Haller JA, Reimann JD, Greene WL, Shams N (2005) Maximum tolerated dose of a humanized anti-vascular endothelial growth factor antibody fragment for treating neovascular age-related macular degeneration. Ophthalmology 112:1048–1053
16. Rosenfeld PJ, Fung AE, Puliafito CA (2005) Optical coherence tomography findings after an intravitreal injection of bevacizumab (avastin) for macular edema from central retinal vein occlusion. Ophthalmic Surg Lasers Imaging 36:336–339
17. Avery RL, Pieramici DJ, Rabena MD, Castellarin AA, Nasir MA, Giust MJ (2006) Intravitreal bevacizumab (Avastin) for neovascular age-related macular degeneration. Ophthalmology 113:363–372
18. Heier JS, Antoszyk AN, Pavan PR, Leff SR, Rosenfeld PJ, Ciulla TA, Dreyer RF, Gentile RC, Sy JP, Hantsbarqer G, Shams N (2006) Ranibizumab for treatment of neovascular age-related macular degeneration: a phase I/II multicenter, controlled, multidose study. Ophthalmology 113:633
19. Jager RD, Aiello LP, Patel SC, Cunningham ET Jr (2004) Risks of intravitreous injection: a comprehensive review. Retina 24:676–698

A novel method of culturing human oral mucosal epithelial cell sheet using post-mitotic human dermal fibroblast feeder cells and modified keratinocyte culture medium for ocular surface reconstruction

Yoshinori Oie,[1,2] Ryuhei Hayashi,[1] Ryo Takagi,[3] Masayuki Yamato,[3] Hiroshi Takayanagi,[4] Yasuo Tano,[2] Kohji Nishida[1]

[1]Department of Ophthalmology and Visual Science, Tohoku University Graduate School of Medicine, Sendai, Japan
[2]Department of Ophthalmology, Osaka University Medical School, Suita, Japan
[3]Institute of Advanced Biomedical Engineering and Science, Tokyo Women's Medical University, Tokyo, Japan
[4]Translational Research Center, Tohoku University, Sendai, Japan

Correspondence to
Dr Kohji Nishida, Department of Ophthalmology and Visual Science, Tohoku University Graduate School of Medicine, Sendai 980-8574, Japan; knishida@oph.med.tohoku.ac.jp)

Accepted 20 February 2010
Published Online First
10 June 2010

ABSTRACT

Background/aims To cultivate human oral mucosal epithelial cell sheets with post-mitotic human dermal fibroblast feeder cells and modified keratinocyte culture medium for ocular surface reconstruction.

Methods Human oral mucosal epithelial cells obtained from three healthy volunteers were cultured with x-ray-treated dermal fibroblasts (fibroblast group) and NIH/3T3 feeder layers (3T3 group) on temperature-responsive culture dishes. Media were supplemented using clinically approved products. Colony-forming efficiency was determined in both groups. Histological and immunohistochemical analyses were performed for cell sheets. Cell viability and purity of cell sheets were evaluated by flow cytometry.

Results Colony-forming efficiency in the fibroblast group was similar to that in the 3T3 group. All cell sheets were well stratified and harvested successfully. The expression patterns of keratin 1, 3/76, 4, 10, 12, 13, 15, ZO-1 and MUC16 were equivalent in both groups. The percentage of p63-positive cells in the fibroblast group (46.1±4.2%) was significantly higher than that in the 3T3 group (30.7±7.6%) ($p=0.038$, t test). The cell viability and purity were similar between the two groups.

Conclusion This novel culture method using dermal fibroblasts and pharmaceutical agents provides a safe cell processing system without xenogenic feeder cells for ocular surface reconstruction.

Tissue-engineered cell sheets composed of autologous oral mucosal epithelium have been successfully used to reconstruct eyes affected with severe ocular surface disorders.[1 2] However, it is possible that murine fibroblast feeder layers used for human transplantation can transmit murine diseases. In addition, it has been reported that human embryonic stem cells cultured on mouse feeder layers generate immunogenic non-human sialic acid.[3] Therefore, a new processing method that does not use animal-derived material should be developed to avoid this problem.

The use of human adipose tissue-derived and bone marrow-derived mesenchymal stem cells is reported to generate transplantable epithelial cell sheets.[4 5] The risks associated with xenogenic feeder layers can be avoided with these methods. However, the harvesting of adipose tissue or bone marrow is invasive; therefore, an alternative cell source for feeder layers is required for autologous cell therapy.

Dermal fibroblasts have been used as a feeder layer to culture skin keratinocytes,[6 7] and dermal fibroblast can be easily cultured.[8] It is thus thought that dermal fibroblasts can be utilised as an alternative candidate for mesenchymal stem cells or NIH/3T3 cells in culturing oral mucosal epithelial cells.

The supplements in conventional keratinocyte culture medium (KCM) are reagents used for laboratory research. The laboratory-grade supplements in KCM should be replaced with pharmaceutical products approved by the Ministry of Health, Labour and Welfare for clinical application. Modified KCM, which adopted the use of clinical agents as culture supplements, was equally as efficient as conventional KCM in the fabrication of canine, transplantable, stratified epithelial cell sheets.[9]

In particular, we investigated a novel culture method of human oral mucosal epithelial cell sheets using post-mitotic human dermal fibroblast feeder cells and modified KCM with clinically approved supplements.

MATERIALS AND METHODS

Preparation of feeder layers

Human dermal tissues were obtained from three healthy volunteers who provided written informed consent. Human tissue was handled according to the Declaration of Helsinki.

Dermal fibroblasts were cultured using the explant procedure.[8] To prepare feeder layers, human dermal fibroblasts were lethally irradiated with 40 Gly and then trypsinised and seeded onto tissue culture dishes (60 mm diameter; BD Biosciences, San Diego, California, USA) at a density of 5×10^3 cells/cm^2 (fibroblast group). As a positive control, lethally irradiated NIH/3T3 cells were prepared at a density of 2×10^4 cells/cm^2 (3T3 group).

Reverse transcription PCR

Total RNA was obtained from human dermal fibroblasts and NIH/3T3 cells using the GenElute mammalian total RNA kit (Sigma, St Louis, Missouri, USA). Reverse transcription was performed with the SuperScript First-Strand Synthesis System for reverse transcription PCR (Invitrogen, Carlsbad, California, USA), according to the manufacturer's suggested protocol, and cDNA was used as the template for PCR. The reverse transcription PCR thermocycle programme consisted of an initial step at 94°C for 5 min and 30 cycles at 94°C for 30 s and 58°C for 30 s and 72°C

for 30 s (PCR Thermal Cycler MP; Takara, Shiga, Japan). The primer pairs are shown in table 1.

Preparation of modified KCM

Modified KCM was supplemented with clinically approved products. The medium consisted of Dulbecco's modified eagle medium and Ham's F12 medium (Gibco-Invitrogen, Carlsbad, California, USA) at a 3:1 ratio, supplemented with 10% autologous human serum, 5 μg/ml insulin (humulin; Eli Lilly, Indianapolis, Indiana, USA), 2 nM triiodothyronine (thyronamin; Takeda, Osaka, Japan), 0.4 μg/ml hydrocortisone (saxizon; Kowa, Tokyo, Japan), 100 nM L-isoproterenol (proternol; Kowa), 2 mM L-glutamine (Gibco), 10 ng/ml epidermal growth factor (Higeta Shoyu, Chiba, Japan), and 40 μg/ml gentamicin (gentacin; Schering-Plough, Kenilworth, New Jersey, USA).

Oral mucosal epithelial cell culture

Human oral mucosal epithelial tissues were obtained from the same three healthy volunteers, respectively. Therefore, we performed the comparison of the two feeder layers three times in the current study. After the oral cavity of each volunteer was sterilised with topical povidone-iodine, a 3×3 mm specimen of oral mucosal tissue was surgically excised from the interior buccal mucosal epithelium under local anaesthesia with propitocaine. Oral mucosal epithelial cells were collected by removing all epithelial layers after treatment with dispase II (2.4 U/ml; Invitrogen), at 4°C for 4 h. Separated epithelial layers were treated with trypsin-EDTA (Invitrogen), and resuspended cells were plated on temperature-responsive culture inserts (CellSeed, Tokyo, Japan) at an initial cell density of 2.0×10^5 cells/23 mm insert, with feeder cells separated by cell culture inserts.[1] The cells were cultured for 14–17 days.

For colony-forming assays, 3000 or 5000 primary oral mucosal epithelial cells were seeded onto culture dishes (60 mm diameter; BD Biosciences) with irradiated feeder layers. After cultivation for 10–12 days, dishes were fixed and stained with rhodamine B. Colony-forming efficiency was defined as the ratio of the number of colonies to the number of cells inoculated. Colony size was also calculated using scanned photos of stained dishes with Axio Vision LE (Carl Zeiss, Jena, Germany).

Table 1 Primer sequences

Gene	Primer sequence (5′→3′)	Product size (bp)
hPTN	Forward: AGAGGACGTTTCCAACTCAA	551
	Reverse: TATGTTCCACAGGTGACATC	
hEPR	Forward: AGGAGGATGGAGATGCTCTG	498
	Reverse: TCAGACTTGCGGCAACTCTG	
hCC	Forward: TCCTCTCTATCTAGCTCCAG	500
	Reverse: TCCTGACAGGTGGATTTCGA	
hHGF	Forward: GCCTGAAAGATATCCCGACA	523
	Reverse: TTCCATGTTCTTGTCCCACA	
hKGF	Forward: AGGCTCAAGTTGCACCAGGCA	495
	Reverse: TGTGTGTCGCTCAGGGCTGGA	
hShh	Forward: CGGAGCGAGGAAGGGAAAG	262
	Reverse: TTGGGGATAAACTGCTTGTAGGC	
hIGF1a	Forward: ATGCACACCATGTCCTC	390
	Reverse: CATCCTGTAGTTCTTGTTTC	
hN-cad	Forward: ATGCTGACGATCCCAATG	317
	Reverse: GATGTCTACCCTGTTCTCA	
hGAPDH	Forward: ACCACAGTCCATGCCATCAC	452
	Reverse: TCCACCACCCTGTTGCTGTA	
mPTN	Forward: GGACCTCTGCAAGCCAAAAAA	317
	Reverse: GCACTCAGCTCCAAACTGCTTC	
mEPR	Forward: AGCTGCACCGAGAAAGAAGGA	318
	Reverse: AGAAGTGCTCACATCGCAGACC	
mCC	Forward: AGCTCGTGGCTGGAGTGAACTA	343
	Reverse: CCTGCAGCAGCTCCTTTACTGT	
mHGF	Forward: GGTGAAAGCTACAGAGGTCCCA	314
	Reverse: ATGGTATTGCTGGTTCCCCTG	
mKGF	Forward: CGAGGCAGACAGCAGACACGG	504
	Reverse: GTGTCGCTCGGGGCTGGAAC	
mShh	Forward: CCCAAAAAGCTGACCCCTTTAG	335
	Reverse: TCCACTGCTCGACCCTCATAGT	
mIGF1a	Forward: TATGGCTCCAGCATTCGGA	319
	Reverse: GCGGTGATGTGGCATTTTCT	
mN-cad	Forward: AGAGGGATCAAAGCCTGGGACGTAT	360
	Reverse: TCCACCCTGTTCTCAGGGACTTCTC	
mGADPH	Forward: ATCACTGCCACCCAGAAGACTG	325
	Reverse: TGCTGTTGAAGTCGCAGGAGA	

CC, cystatin C; EPR, epiregulin; GAPDH, glyceraldehydes-3-phosphate dehydrogenase; h, human; HGF, hepatocyte growth factor; IGF1a, insulin-like growth factor 1a; KGF, keratinocyte growth factor; m, mouse; N-cad, N-cadherin; PTN, pleiotrophin; Shh, sonic hedgehog.

Cell morphology

Cultured epithelial cells were observed under a phase contrast microscope, and microphotographs were taken at 100-fold magnification (Axiovert40; Carl Zeiss, Jena, Germany) to examine cell morphological aberrations and deficits.

Sheet recovery test

After examination with phase contrast microscopy, cultured epithelial cells were subjected to incubation at 20°C for 30 min. Then, a donut-shaped support membrane (18 mm outer diameter, 10 mm inner diameter, polyvinylidene difluoride; Millipore, Bedford, Massachusetts, USA) was placed on the epithelial cells. Finally, cells were challenged with harvesting in the presence of support membranes. Harvested epithelial cell sheets were divided into two parts. Half of the cell sheets were subjected to flow cytometry and the other half were subjected to histological analyses.

Cell viability and epithelial cell purity

Cell viability was evaluated with a dye exclusion test. An aliquot of cell suspension was incubated in Dulbecco's modified eagle medium with 7-aminoactinomycin D (BD Biosciences) staining at room temperature for 10 min, and subjected to flow cytometry (FACS Calibur; BD Biosciences).

After trypsin-EDTA treatment, an aliquot of the cell suspension was centrifuged, fixed and permeabilised with the Cytofix/Cytoperm kit (BD Biosciences) according to the manufacturer's protocol. Then, the cell suspension was split into two tubes, and incubated with either a FITC-conjugated anti-pancytokeratin IgG2a antibody (clone Pan1-8; Progen, Heidelberg, Germany) or a FITC-conjugated mouse control IgG2a antibody (Santa Cruz Biotechnology, Santa Cruz, California, USA) at room temperature for 60 min. After being washed twice with PBS, nuclei were stained with 7-aminoactinomycin D and the cells were examined by flow cytometry.

H&E staining and immunofluorescence analyses

The portion of cell sheets to be used in histological analyses was divided into two quadrants. One quadrant was fixed with formalin and embedded in paraffin. H&E staining was performed to observe the morphology and degree of stratification of the cultured epithelial cells. Microphotographs were taken with a light microscope (BZ-9000, Keyence, Osaka, Japan).

The other quadrant of cell sheets was embedded in Tissue-Tek OCT compound (Sakura Seiki, Tokyo, Japan) and processed into

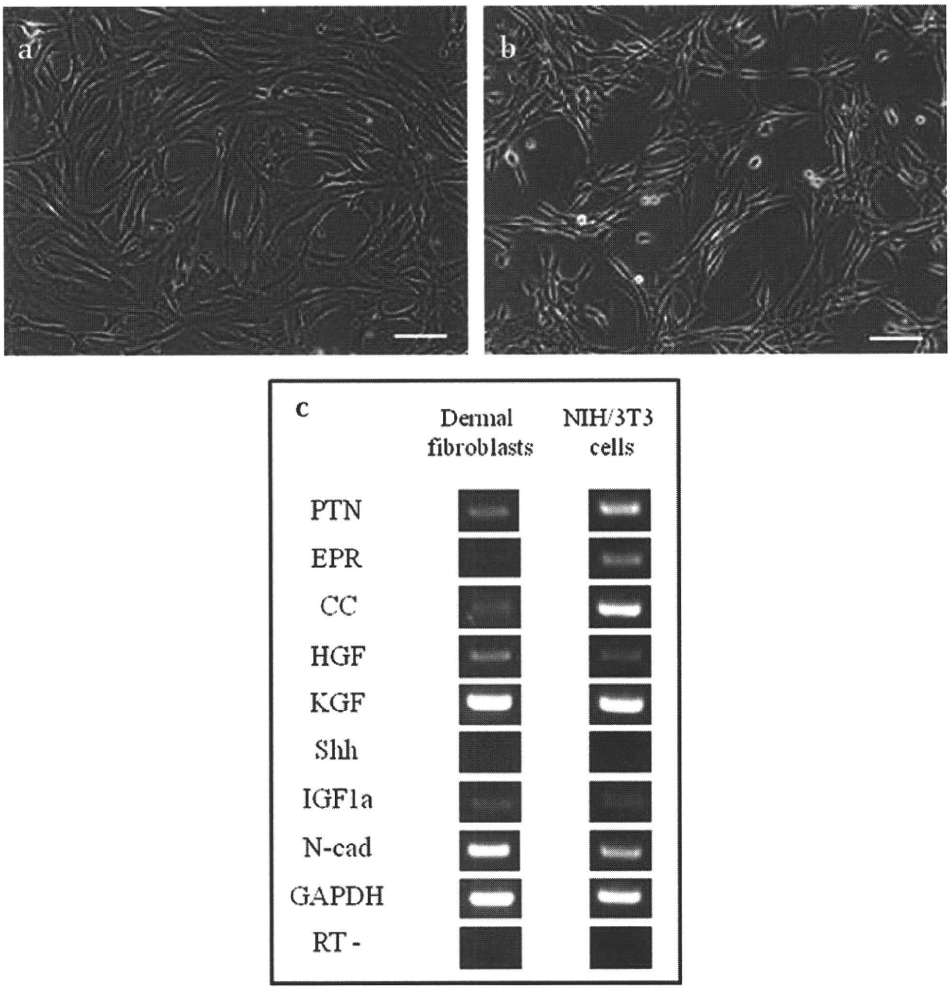

Figure 1 Feeder layers. Human dermal fibroblasts (A) and NIH/3T3 cells (B) were examined using phase-contrast microscopy. Gene expression was analysed by reverse transcription PCR. Both human dermal fibroblasts and NIH/3T3 cells expressed many factors for the maintenance of stem/progenitor cells and the growth of epithelial cells (C). Scale bars: 100 μm (A, B). CC, cystatin C; EPR, epiregulin; GAPDH, glyceraldehyde-3-phosphate dehydrogenase; HGF, hepatocyte growth factor; IGF1a, insulin-like growth factor 1a; KGF, keratinocyte growth factor; N-cad, N-cadherin; PTN, pleiotrophin; Shh, sonic hedgehog.

3-μm thick frozen sections. Cryosections from the cell sheets were immunostained with monoclonal antibodies against keratin 1 (K1, LHK1; Abcam, Cambridge, UK), keratin 3/76 (K3/76, AE5; Progen), keratin 4 (K4, 6B10; Abcam), keratin 10 (K10, DE-K10; DakoCytomation, Glostrup, Denmark), keratin 13 (K13, 1C7; American Research Products, Belmont, Massachusetts, USA), keratin 15 (K15, LHK15; Millipore), p63 (4A4; Santa Cruz Biotechnology), ZO-1 (1A12; Zymed, South San Francisco, California, USA), MUC16 (Ov185; Abcam), a polyclonal antibody against keratin 12 (K12, L-15; Santa Cruz Biotechnology), followed by incubation with Alexa488-labelled secondary antibodies (Molecular Probes, Eugene, Oregon, USA). Nuclei were co-stained with Hoechst 33342 (Sigma), and the cell sheets were mounted with PermaFluor (Beckman Coulter, Miami, Florida, USA). Slides were observed using confocal laser scanning microscopy (LSM-710; Carl Zeiss). The same concentration of corresponding normal, non-specific IgG was used as negative control. The percentage of p63 and K15-positive cells in each cultured cell sheet was calculated.

Statistical analysis

Data were analysed using t tests; $p<0.05$ was considered statistically significant.

RESULTS

Human dermal fibroblasts had morphological characteristics similar to those of NIH/3T3 cells (figure 1A, B). The gene expression pattern of dermal fibroblasts was similar to that of NIH/3T3 cells (figure 1c). Although dermal fibroblasts did not express epiregulin (EPR), other genes including pleiotrophin (PTN), cystatin C (CC), hepatocyte growth factor (HGF), keratinocyte growth factor (KGF), insulin-like growth factor 1a (IGF1a) and N-cadherin (N-cad) were expressed by both dermal fibroblasts and NIH/3T3 cells.

Colony-forming assays revealed that human dermal fibroblasts as well as NIH/3T3 cells are able to support the ex-vivo expansion of oral mucosal epithelial cells (figure 2A–D). The mean colony-forming efficiency of the primary cultures was 1.5±0.8% in the fibroblast group and 2.3±0.8% in the 3T3 group (mean±SD, n=3) (figure 2E), and the difference was not statistically significant (p=0.266, t test). The colony size in the fibroblast group (15.0±11.5 mm^2) was larger than that in the 3T3 group (6.4±2.1 mm^2). However, the difference was not statistically significant (p=0.271, t test).

Oral mucosal epithelial cell sheets were successfully cultured with human dermal fibroblasts and NIH/3T3 cells (figure 3A, B), and all of the cell sheets were successfully harvested by reducing the temperature to 20°C for 30 min. Therefore, all of the cell sheets passed the recovery test. The harvested cell sheets in both groups, flattened at their basal and apical surfaces, were composed of four to five layers of small basal cells, flattened middle cells and polygonal flattened superficial cells (figure 3C, D).

Immunofluorescence analyses revealed that cell sheets in both groups have a similar marker expression pattern (figure 4). K3/76, a marker for corneal and oral mucosal differentiated epithelial cells,[10] was positive in both groups. K12,

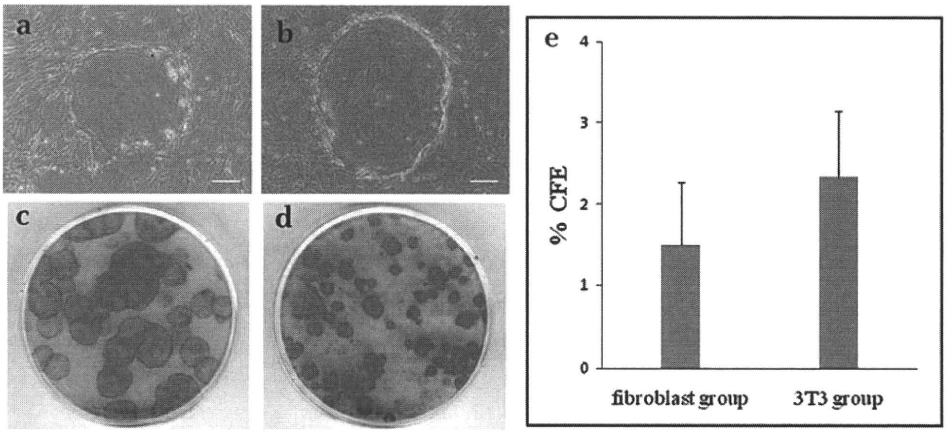

Figure 2 Colony-forming assay. Human dermal fibroblasts (A) as well as NIH/3T3 cells (B) supported the ex-vivo expansion of human oral mucosal epithelial cells. Cells were cultured for approximately 10 days, followed by fixation and staining with rhodamine B (C, dermal fibroblasts; D, NIH/3T3 cells). Colony-forming efficiency (CFE) was calculated, and no statistically significant differences were found between the human dermal fibroblasts and NIH/3T3 cells (E). Scale bars 100 μm (A, B).

a corneal-epithelium-specific marker,[10] was not expressed in either group. Although K4 and K13 are markers for mucosal stratified squamous epithelia,[11 12] only K4 was detected in the superficial cells in both groups. K1 and K10, markers for supra-basal cells in the epidermis,[13] were negative in both groups. ZO-1, a marker of tight junctions,[14] and MUC 16, a membrane associated-mucin specific to ocular surfaces, were expressed in both groups.

p63, which has been proposed to be a corneal epithelial stem/progenitor cell marker,[15] was expressed in the basal cells of both groups (figure 5A, B). The percentage of p63-positive cells in the fibroblast group (46.1±4.2%) was significantly higher than that in the 3T3 group (30.7±7.6%) (p=0.038, t test) (figure 5E). K15, a specific basal cell component of the epidermis and other stratified squamous epithelia,[16] was positive in basal cells in both groups (figure 5C, D). There were no significant differences between the percentages of K15-positive cells in the fibroblast group (24.0±3.7%) and the 3T3 group (20.6±2.5%) (p=0.257, t test) (figure 5F).

The cell viability of the cultured cell sheets in the fibroblast group and the 3T3 group was 88.7±4.1% and 85.9±3.5%, respectively. The purity of the epithelial cells in the cultured sheets was 98.2±1.9% and 96.3±3.6%, respectively. There were no statistical differences in cell viability (p=0.408, t test) or purity (p=0.466, t test) between the groups.

DISCUSSION

Dermal fibroblasts were shown to express many genes required for the maintenance of epithelial stem/progenitor cells and the proliferation of epithelial cells. Sugiyama *et al*[4] reported the expression of PTN, EPR, CC, HGF, KGF and IGF1a by human mesenchymal stem cells. In the current study, human dermal fibroblasts were confirmed to express N-cadherin in addition to these factors. The colony-forming efficiency with human dermal fibroblasts was similar to that with NIH/3T3 cells, and a colony-forming assay revealed that human dermal fibroblasts can expand oral mucosal epithelial cells well. In addition, immuno-fluorescence analyses revealed that cell sheets cultured with human dermal fibroblasts, as well as with NIH/3T3 cells, expressed markers such as K3/76, ZO-1, MUC16, p63, and K15. Moreover, cell sheets cultured with human dermal fibroblasts contained more p63-positive cells than those cultured with NIH/3T3 cells. Therefore, it was suggested that human dermal fibroblasts can maintain stem/progenitor cells in expansion more efficiently than NIH/3T3 cells.

The cultivation of epithelial cells with 3T3 feeder layers has been already established.[18] Also, a number of investigators has reported positive results for clinical treatments with cultured epithelial cells using 3T3 feeder layers.[1 18 19] However, 3T3 cells have the potential risk of transmitting murine infectious diseases. The use of xeno-free feeder cells, especially autologous

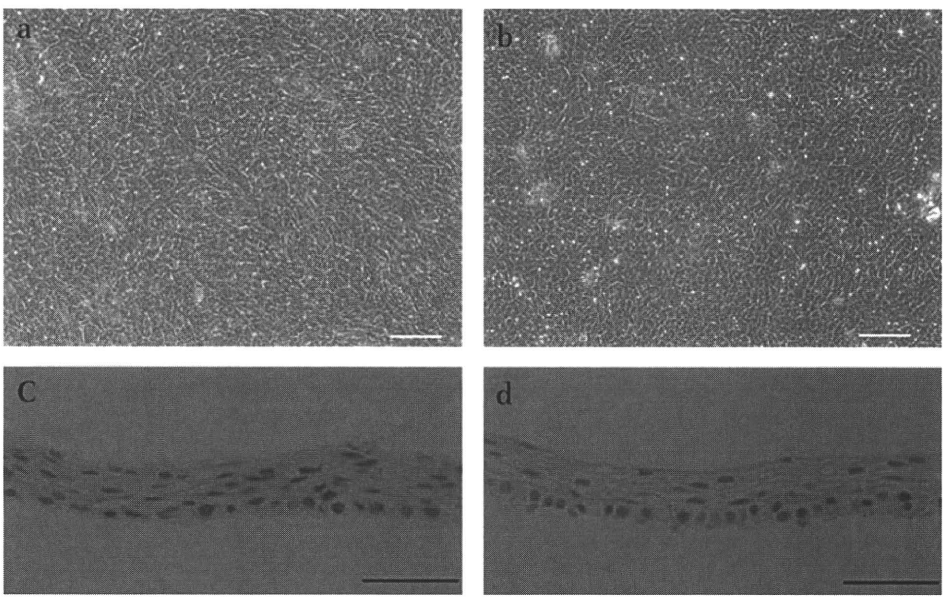

Figure 3 Human oral mucosal epithelial cell sheets. Examination of cell morphology was performed using phase-contrast microscopy (A, dermal fibroblasts; B, NIH/3T3 cells) and H&E staining (c, dermal fibroblasts; d, NIH/3T3 cells). Scale bars 100 μm (A, B), 50 μm (C, D).

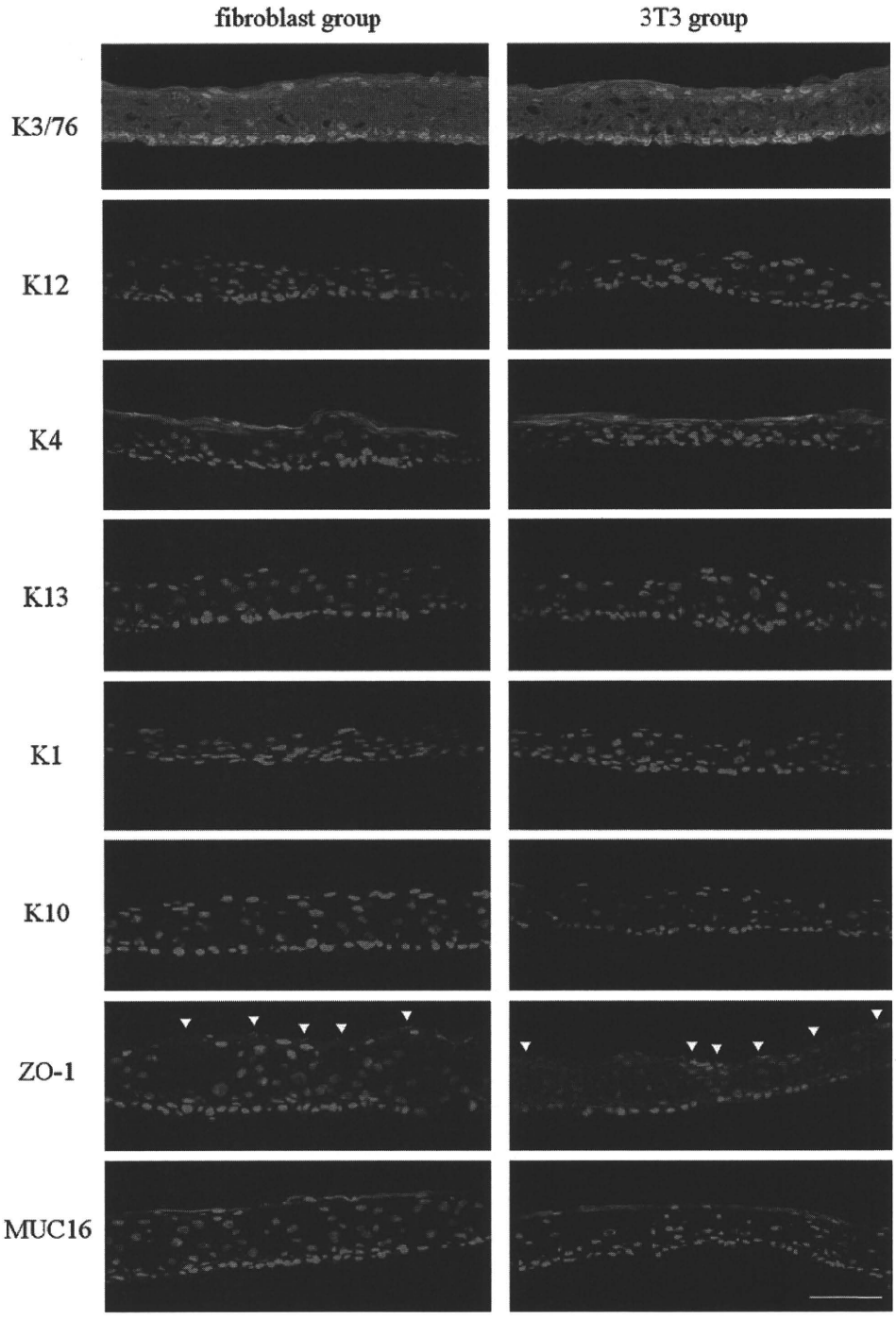

Figure 4 Immunohistochemical analyses of human oral mucosal epithelial cell sheets. Staining of human oral mucosal epithelial cell sheets cultured with dermal fibroblasts and NIH/3T3 cells with anti-keratin 3/76 (K3/76), anti-keratin 12 (K12), anti-keratin 4 (K4), anti-keratin 13 (K13), anti-keratin 1 (K1), anti-ZO-1 and anti-MUC16 antibodies. Nuclei were co-stained with Hoechst 33342. ZO-1 expression is marked with arrows. Scale bars 50 μm.

feeder layers, can prevent this problem. Although human adipose tissue-derived or bone marrow-derived mesenchymal stem cells can be used to generate transplantable epithelial cell sheets, dermal fibroblasts can be obtained with much less invasion to patients. Therefore, dermal fibroblasts are more desirable as an autologous feeder cell source than mesenchymal stem cells. Whereas the colony-forming efficiency of human limbal epithelial cells was 1.9±1.8% with bone marrow-derived mesenchymal stem cells,[5] that of human oral mucosal epithelial cells was 1.5±0.8% with human dermal fibroblasts in the current study. The colony-forming efficiency in these two reports cannot be compared directly, because of differences in the cultured epithelial cell type, media and sera. However, both feeder layers are thought to be able to generate transplantable epithelial cell sheets.

A xeno-free culture method of keratinocytes derived from skin using human dermal fibroblast has already been reported.[7] Therefore, it is well known that human dermal fibroblasts have a feeder effect on keratinocytes. Here, we cultured oral mucosal epithelial cells using human dermal fibroblast feeder layers. We are planning to use the cultured cell sheets for ocular reconstruction in future experiments. Zakaria *et al*[20] recently reported a new culture and transplantation method of limbal epithelial cells without xenogenic materials. If oral mucosal epithelial cells

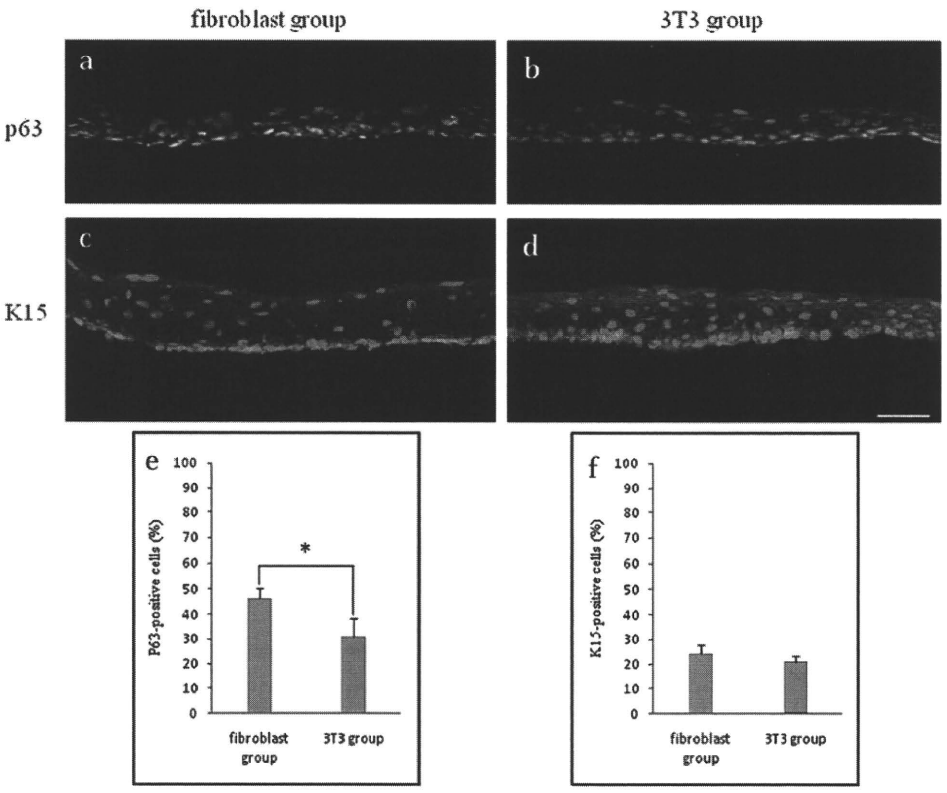

Figure 5 Analyses of human oral mucosal epithelial cell sheets for stem/progenitor markers. Anti-p63 staining (A, B) and anti-keratin 15 (K15) staining (C, D) of human oral mucosal epithelial cell sheets cultured with dermal fibroblasts and NIH/3T3 cells. Nuclei were co-stained with Hoechst 33342. Scale bar 50 μm. The percentage of p63-positive cells in the cell sheets cultured with dermal fibroblasts was significantly higher than that in cell sheets cultured with NIH/3T3 cells (E). The percentage of K15-positive cells was not significantly different between the groups (F). *$p<0.05$, t test.

can be cultured successfully, this method can also be an alternative to the method using 3T3 cells.

We recently developed a validation system for tissue-engineered epithelial cell sheets to be used in corneal regenerative medicine.[21] There has been no other established evaluation method for epithelial cell sheets before transplantation to date. However, the quality of cell sheets for clinical use can be standardised even in different facilities. We evaluated cell sheets using our validation method and obtained positive results. We thus believe that the oral mucosal epithelial cell sheets cultured with this method can be successfully used for ocular reconstruction.

It was previously reported that fibroblasts can affect the phenotypic characterisation of keratinocytes in co-culture.[22 23] However, epithelial cell sheets cultivated in the current study did not express K1 or K10, markers for suprabasal cells in the epidermis. Therefore, we propose that the phenotypic characterisation of keratinocytes cultured in the current study did not reflect that of the epidermis.

We also demonstrated that modified KCM worked well to generate oral mucosal epithelial cell sheets. Many methods using cholera toxin have been reported for the cultivation of human corneal or oral mucosal epithelial cells and human epidermal keratinocytes.[17 18 24] Agents known to increase the level of cellular cyclic AMP, including cholera toxin and isoproterenol, have been reported to increase the growth of colonies of cultured human epidermal cells and keratinocytes derived from other stratified squamous epithelia.[25] We also demonstrated the effectiveness of modified KCM with isoproterenol in the current study.

In conclusion, our novel culture system with post-mitotic human dermal fibroblast feeder cells with clinically approved products is effective and safe. Therefore, this system can be used as an alternative cultivation method for human oral mucosal epithelial cell sheets.

Funding This study was funded by the Ministry of Health Labor and Welfare, and the Ministry of Education, Culture, Sports, Science and Technology in Japan.

Competing interests None.

Ethics approval This study was conducted with the approval of the institutional review board of Tohoku University School of Medicine.

Provenance and peer review Not commissioned; externally peer reviewed.

REFERENCES

1. **Nishida K,** Yamato M, Hayashida Y, *et al*. Corneal reconstruction with tissue-engineered cell sheets composed of autologous oral mucosal epithelium. *N Engl J Med* 2004;**351**:1187–96.
2. **Nakamura T,** Inatomi T, Sotozono C, *et al*. Transplantation of cultivated autologous oral mucosal epithelial cells in patients with severe ocular surface disorders. *Br J Ophthalmol* 2004;**88**:1280–4.
3. **Martin MJ,** Muotri A, Gage F, *et al*. Human embryonic stem cells express an immunogenic nonhuman sialic acid. *Nat Med* 2005;**11**:228–32.
4. **Sugiyama H,** Maeda K, Yamato M, *et al*. Human adipose tissue-derived mesenchymal stem cells as a novel feeder layer for epithelial cells. *J Tissue Eng Regen Med* 2008;**2**:445–9.
5. **Omoto M,** Miyashita H, Shimmura S, *et al*. The use of human mesenchymal stem cell-derived feeder cells for the cultivation of transplantable epithelial sheets. *Invest Ophthalmol Vis Sci* 2009;**50**:2109–15.
6. **Bell E,** Ivarsson B, Merrill C. Production of a tissue-like structure by contraction of collagen lattices by human fibroblasts of different proliferative potential in vitro. *Proc Natl Acad Sci U S A* 1979;**76**:1274–8.
7. **Bullock AJ,** Higham MC, MacNeil S. Use of human fibroblasts in the development of a xenobiotic-free culture and delivery system for human keratinocytes. *Tissue Eng* 2006;**12**:245–55.
8. **Hayflick L,** Moorhead PS. The serial cultivation of human diploid cell strains. *Exp Cell Res* 1961;**25**:585–621.
9. **Takagi R,** Yamato M, Yang J. Preparation of keratinocyte culture medium for clinical applications for regenerative medicine. *J Tissue Eng Regen Med 2010*; In press.
10. **Schermer A,** Galvin S, Sun TT. Differentiation-related expression of a major 64K corneal keratin in vivo and in culture suggests limbal location of corneal epithelial stem cells. *J Cell Biol* 1986;**103**:49–62.
11. **Moll R,** Franke WW, Schiller DL, *et al*. The catalog of human cytokeratins: patterns of expression in normal epithelia, tumors and cultured cells. *Cell* 1982;**31**:11–24.
12. **Cooper D,** Schermer A, Sun TT. Classification of human epithelia and their neoplasms using monoclonal antibodies to keratins: strategies, applications, and limitations. *Lab Invest* 1985;**52**:243–56.
13. **Fuchs E,** Green H. Changes in keratin gene expression during terminal differentiation of the keratinocyte. *Cell* 1980;**19**:1033–42.

14. **Hayashida Y,** Nishida K, Yamato M, *et al*. Ocular surface reconstruction using autologous rabbit oral mucosal epithelial sheets fabricated ex vivo on a temperature-responsive culture surface. *Invest Ophthalmol Vis Sci* 2005;**46**: 1632–9.
15. **Pellegrini G,** Dellambra E, Golisano O, *et al*. p63 identifies keratinocyte stem cells. *Proc Natl Acad Sci U S A* 2001;**98**:3156–61.
16. **Moll I,** Troyanovsky SM, Moll R. Special program of differentiation expressed in keratinocytes of human haarscheiben: an analysis of individual cytokeratin polypeptides. *J Invest Dermatol* 1993;**100**:69–76.
17. **Rheinwald JG,** Green H. Serial cultivation of strains of human epidermal keratinocytes: the formation of keratinizing colonies from single cells. *Cell* 1975;**6**: 331–43.
18. **Pellegrini G,** Traverso CE, Franzi AT, *et al*. Long-term restoration of damaged corneal surfaces with autologous cultivated corneal epithelium. *Lancet* 1997;**349**: 990–3.
19. **Nishida K,** Yamato M, Hayashida Y, *et al*. Functional bioengineered corneal epithelial sheet grafts from corneal stem cells expanded ex vivo on a temperature-responsive cell culture surface. *Transplantation* 2004;**77**:379–85.
20. **Zakaria N,** Koppen C, Van Tendeloo V, *et al*. Standardized limbal epithelial stem cell graft generation and transplantation. *Tissue Eng Part C Methods 2010*. Published Online First: 4 February 2010. doi:10.1089/ten.tec.2009.0634.
21. **Hayashi R,** Yamato M, Takayanagi H, *et al*. Validation system of tissue engineered epithelial cell sheets for corneal regenerative medicine. *Tissue Eng Part C Methods 2010*; Published Online First: 13 April 2010. doi:10.1089/ten.tec.2009.0277.
22. **Kideryova L,** Lacina L, Dvorankova B, *et al*. Phenotypic characterization of human keratinocytes in coculture reveals differential effects of fibroblasts from benign fibrous histiocytoma (dermatofibroma) as compared to cells from its malignant form and to normal fibroblasts. *J Dermatol Sci* 2009;**55**:18–26.
23. **Blazejewska EA,** Schlotzer-Schrehardt U, Zenkel M, *et al*. Corneal limbal microevironment can induce transdifferentiation of hair follicle stem cells into corneal epithelial-like cells. *Stem Cells* 2009;**27**:642–52.
24. **Yokoo S,** Yamagami S, Usui T, *et al*. Human corneal epithelial equivalents for ocular surface reconstruction in a complete serum-free culture system without unknown factors. *Invest Ophthalmol Vis Sci* 2008;**49**:2438–43.
25. **Green H.** Cyclic AMP in relation to proliferation of the epidermal cell: a new view. *Cell* 1978;**15**:801–11.

Jpn J Ophthalmol 2010;54:494–498
DOI 10.1007/s10384-010-0861-6

LABORATORY INVESTIGATION

Chromosomal Sharing in Atypical Cases of Gelatinous Drop-like Corneal Dystrophy

Motokazu Tsujikawa, Naoyuki Maeda, Kaoru Tsujikawa, Yuichi Hori, Tomoyuki Inoue, and Kohji Nishida

Department of Ophthalmology, Osaka University Graduate School of Medicine, Osaka, Japan

Abstract

Purpose: To present the phenotypic variability both among and within families in Japanese gelatinous drop-like corneal dystrophy (GDLD), and to study the genetic background of the variability.

Methods: Four Japanese families who suffer from bilateral corneal amyloidoses were studied by a molecular genetic method. All families included a patient whose clinical features alone could not be used to diagnose GDLD. In one family, obvious clinical differences were observed between the two members who were patients. Three families had members who suffered from atypical amyloidoses that had not been initially diagnosed as GDLD. For their final diagnoses and for the investigation of the genetic background of these phenotypes, the sequences of the entire *TACSTD2* gene and the genotypes of some polymorphic markers close to the *TACSTD2* gene were studied.

Results: Genetic analysis revealed that all the patients possessed a homozygous Q118X mutation in *TACSTD2,* a major founder mutation in Japanese GDLD. There were no differences in the entire sequence of *TACSTD2* in these patients compared with other GDLD patients. Moreover, the genotyping of polymorphic markers near the *TACSTD2* gene revealed that these patients shared the same founder chromosome as well as the *TACSTD2* gene.

Conclusion: In Japanese GDLD patients, phenotypic variability is observed both among and within families in spite of the allelic homogeneity of Q118X. Even in these atypical cases, the patients shared the same chromosomal region, received from a founder. **Jpn J Ophthalmol** 2010;54:494–498 © Japanese Ophthalmological Society 2010

Keywords: founder effect, GDLD, gelatinous drop-like corneal dystrophy, M1S1, TACSTD2

Introduction

Gelatinous drop-like corneal dystrophy (GDLD; OMIM 204870) is one of the most severe corneal dystrophies with autosomal recessive inheritance. In most cases, its clinical features are grayish corneal amyloid elevation and corneal neovascularization, leading to severe visual impairment.[1,2] We previously identified the gene responsible for GDLD, tumor-associated calcium signal transducer 2 (*TACSTD2*, formerly, *M1S1/TROP2/GA733-1*) using positional cloning.[3,4] Molecular analyses have revealed that most Japanese GDLD patients are homozygous for the Q118X mutation in *TACSTD2*, and 90% of GDLD chromosomes possess this founder mutation.[5–7]

Because of its apparent clinical features, in most cases the diagnosis of GDLD is easy. However, clinical variability and atypical cases have been reported.[8] An important question is whether these atypical cases are caused by genetic background differences, including allelic or locus heterogeneities. In this study, we demonstrated phenotypic variability both among and within families and allelic homogeneity of Q118X among them. Moreover, using intragene and close genetic markers, we showed that even among these atypical cases, a common haplotype is present owing to chromosomal sharing from a common ancestor.

Received: December 7, 2009 / Accepted: March 30, 2010
Correspondence and reprint requests to: Motokazu Tsujikawa, Department of Ophthalmology, Osaka University Graduate School of Medicine, Rm E7, 2-2 Yamadaoka, Suita, Osaka 565-0871, Japan
e-mail: moto@ophthal.med.osaka-u.ac.jp

Patients and Methods

Families and Patients

We studied four Japanese families that included individuals suffering from bilateral corneal amyloid deposition and opacity. In three families, the amyloidoses differed from typical GDLD and the patients could not be diagnosed as GDLD only on the basis of their clinical features and examinations. In the fourth family, one member was diagnosed as having GDLD, not by clinical features but by family history. The final diagnoses of GDLD in these families were obtained by the genetic analyses described here. All patients provided written informed consent for this study and procedures followed the tenets of the Declaration of Helsinki. This study was approved by the institutional review board of the Osaka University Medical School.

Mutation Analysis and Genotyping

From each participant, 20 ml of peripheral blood was taken. Genomic DNA was extracted from white blood cells by standard methods.[9] The entire *TACSTD2* gene region, including the 5′ flanking side was amplified by polymerase chain reaction (PCR) with primers GDLD1F (5′-GAG CAGCTTCCCTGTTCTGA-3′) and GDLD11R (5′-CTG CAGTTTGAAGGAAGTTTCC-3′). PCR was carried out in a 20-μl reaction mixture containing 50 ng of genomic DNA, 10 pmol of each primer, 2.0 mM $MgCl_2$, 1 × reaction buffer (Takara, Tokyo, Japan), 150 μM of each dNTP, and 1.0 U of *ExTaq* polymerase (Takara). Samples were amplified in 32 cycles of 30 s at 94°C, 30 s at 60°C, and 30 s at 72°C. PCR products were purified with a QIAquick PCR purification kit (QIAGEN, Valencia, CA, USA) and then sequenced with a Big-Dye Terminator cycle sequencing kit and analyzed using a 377 automated sequencer (Applied Biosystems, Foster City, CA, USA). To confirm the Q118X mutation detected by sequencing, PCR-restriction fragment length polymorphism analysis (RFLP) was performed. The nucleotide alteration introduces a *Mae*I recognition site, so PCR products obtained with the primer set GDLD3F (5′-ACGTGTCCCACCAACAAGAT-3′) and GDLD3R (5′-AGTTCACGCACCAGCACA-3′) were cleaved with *Mae*I and electrophoresed on 12% polyacrylamide gel.

Genotype analysis was performed on three microsatellite markers, D1S220, D1S2700, and D1S2648 near the *TACSTD2* gene, spanning 400 kbp. One PCR primer for each marker was fluorescently labeled with 6-FAM or HEX (Takara Bio, Shiga, Japan). Each PCR was carried out as described above. PCR products were electrophoresed on 4% denaturing polyacrylamide gels for 2 h and analyzed with the 377 automated sequencer. Genescan analysis software (Applied Biosystems) was used to determine allele size.

Results

Case Reports

Family 1

Family 1 was consanguineous and had two male patients. The proband (II-1) is a typical GDLD patient. He suffered from photophobia, lacrimation, and blurred vision in his first decade. Penetrating keratoplasties were performed on his right eye when he was 22 years old and on his left eye when he was 31 years old, in another hospital. As in some of the other patients, recurrence of amyloid deposition required additional excimer laser phototherapeutic keratectomy in his right eye when he was 46 years old. Even on the transplanted corneas, recurrence of numerous bilateral grayish elevated round depositions and superficial neovascularization can be clearly observed (Fig. 1A).

One of his younger brothers (II-3) was first examined at 39 years of age, when the family members were examined for a segregation study of the *TACSTD2* mutation.[4] The elder brother had had surgical interventions in both eyes by age 30, but the younger brother did not show clear clinical manifestations of GDLD at the same age. He had suffered from photophobia for 2 years; however, he did not have any other symptoms and had not been examined by an ophthalmologist. In the center of the cornea, subepithelial opacity and fine depositions were observed; however, neither an elevated gelatinous region nor neovascularization was observed (Fig. 1B). Late fluorescent staining in both eyes suggested deterioration of the barrier function of the corneal epithelium. He did not need any intervention to his corneal region.

Family 2

Family 2 was also consanguineous and had one male patient, a 9-year-old boy who had mild corneal opacity in both eyes that was diagnosed as macular corneal dystrophy by corneal subspecialists of another university hospital. Small, round white droplets were observed at the subepithelial stroma. The droplets clustered and elevated the epithelium in the center of both corneas; however, similar to patient II-3 in family 1, no prominent elevated region or neovascularization was observed (Fig. 2A). In the center of both corneas, superficial punctuate keratitis and late staining of the epithelium were observed.

Family 3

Family 3 was nonconsanguineous and had one 68-year-old female patient. Clusters of fine yellow lipid droplets were observed beneath the corneal epithelium, mainly in the exposed area from the periphery to the center, and created band-shaped lesions on the scarred corneal stroma. These lipid depositions were different from those of typical GDLD.

Jpn J Ophthalmol
Vol 54: 494–498, 2010

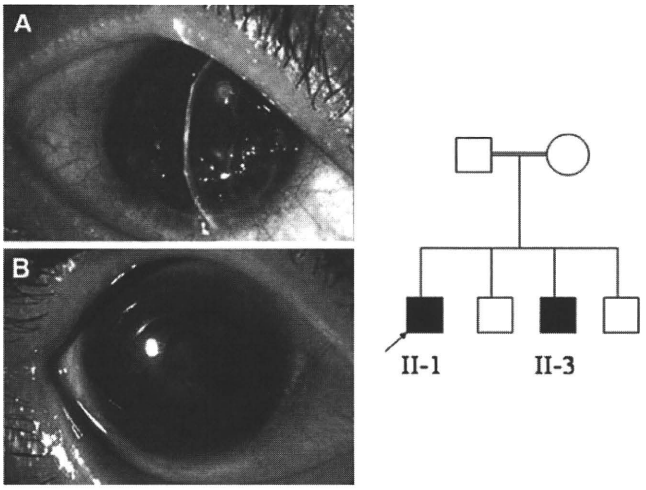

Figure 1A, B. Family 1 shows a phenotypic variability within the family. **A** Right eye of patient II-1 shows typical recurrent gelatinous drop-like corneal dystrophy (GDLD). Best-corrected visual acuity OD was 20/200. **B** Right eye of patient II-3 in family 1. The phenotype is obviously much milder than that of his brother. Best-corrected visual acuity OD was 20/40. Note that there are no elevated gelatinous regions or neovascularization.

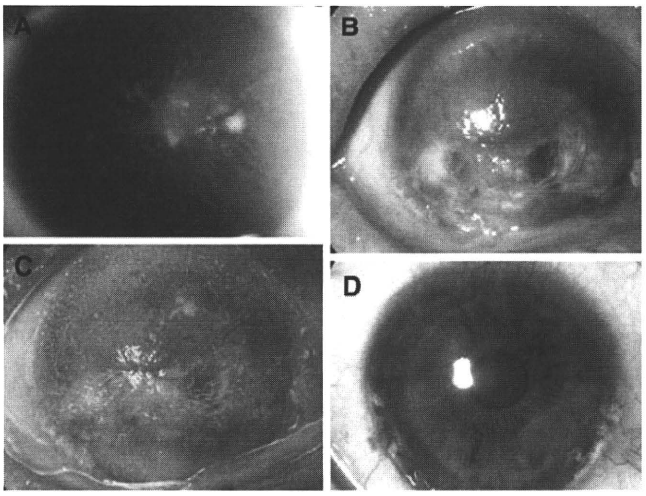

Figure 2A–D. Phenotypic variability among the families. **A** Right eye of the patient in family 2. No prominent elevated regions or neovascularization were observed. Best-corrected visual acuity OD was 20/30. **B** Right eye of the patient in family 3. Note band-shaped yellow fatty deposits and the loss of the palisades of Vogt. Best-corrected visual acuity OD was 20/400. **C** Late fluorescent staining in family 3. **D** Left eye of the patient in family 4. Note band-shaped, lipid-like, yellowish deposition. Best-corrected visual acuity OD was 20/30.

In this case, obvious neovascularization (Fig. 2B) and late fluorescent staining was observed in both eyes (Fig. 2C). On the basis of these clinical examination results, we diagnosed her as having spheroidal corneal degeneration before the genetic analysis.

Family 4

Family 4 is consanguineous and has one 38-year-old male patient who suffered from blurred vision in his first decade. At the corneal facility of another university hospital he was diagnosed with spheroidal corneal degeneration. He underwent lamellar keratoplasty in his left eye at 34 years of age and in his right eye at 36 years. After keratoplasty, the corneal opacity almost completely disappeared except for a subepithelial opacity in the center of the graft. A band-shaped, white deposition in the center of the graft and superficial neovascularization were observed as well (Fig. 2D). Outside the graft, on the peripheral cornea, yellowish deposits that looked like a pinguecula were detected. Late fluorescent staining was also observed in both eyes.

Molecular Genetic Analysis

Sequence and RFLP analysis revealed that all GDLD patients in this study were homozygous for the Q118X mutation (Fig. 3). In families 1 and 2, the Q118X mutation cosegregated with the GDLD phenotype. All of these patients also were homozygous for the D216E polymorphism (data not shown). No other nucleotide alterations were observed, and all sequences from the patients were

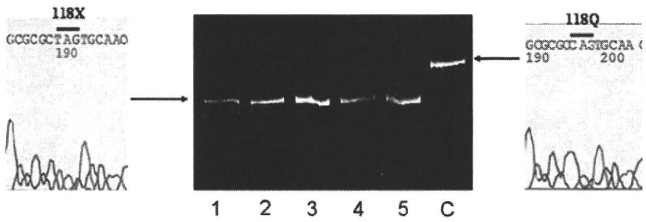

Figure 3. Sequence and restriction fragment length polymorphism analysis of the presented patients. All patients possessed a homozygous Q118X (CAG- > TAG) mutation. *Lanes*: *1*, patient II-1 from family 1; *2*, patient II-3 from family 1; *3*, patient from family 2; *4*, patient from family 3; *5*, patient from family 4; *C*, normal control.

identical. Genotype analysis revealed that all disease chromosomes possessed a 204-bp allele on D1S2752, a 285-bp allele on D1S2648, and a 247-bp allele on D1S220 (Fig. 4). Thus, the haplotype of all disease chromosomes was 204bp-285bp-247bp D1S2752-D1S2648-D1S220).

Discussion

In other corneal dystrophies such as *TGFBI* (formerly βig-h3, transforming growth factor beta-induced gene)-associated inherited corneal dystrophies, apparent genotype–phenotype correlations have been observed.[10–12] For example, granular corneal dystrophy type I is caused mainly by an R555W mutation in *TGFBI*, and Avellino corneal dystrophy by an R124H mutation.[5,11,13] Even varied phenotypes from the same mutation have been reported.[14] We can usually diagnose these dystrophies easily following a clinical

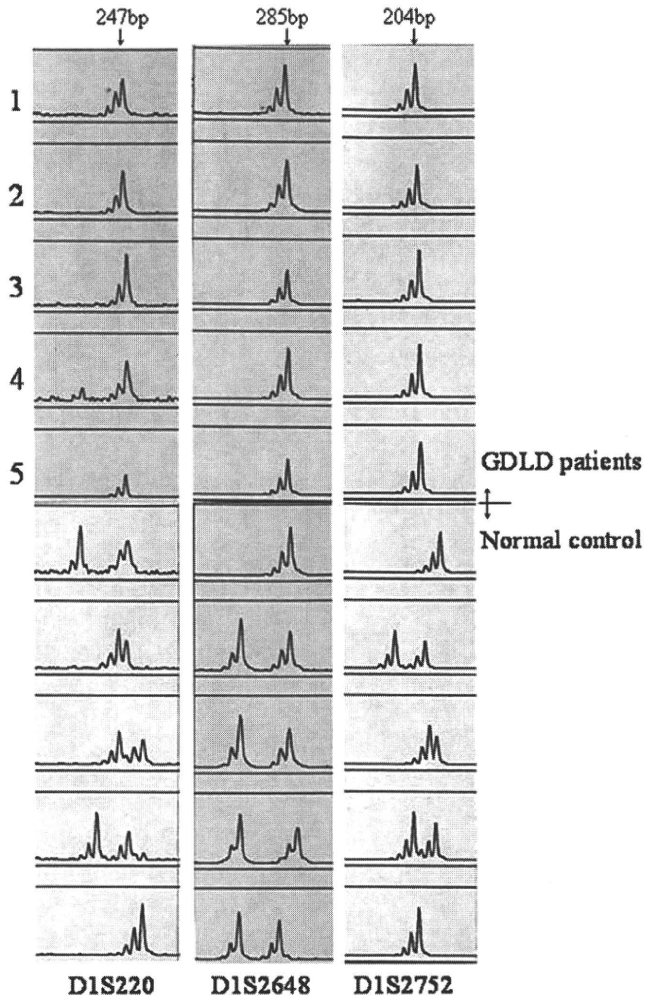

Figure 4. Genotype analysis of the markers flanking the*TACSTD2*. *Top five rows,* analysis results of the GDLD patients: *1*, Patient II-1 from family 1; *2*, patient II-3 from family 1; *3*, patient from family 2; *4*, patient from family 3; *5*, patient from family 4. All patients are homozygotes, and all haplotypes of the disease chromosome were 204bp-285bp-247bp (D1S2752-D1S2648-D1S220). *Bottom five rows,* analysis results of five normal Japanese controls with apparent heterozygosity at these markers.

examination only. In *TGFBI*-associated dystrophies, genetics is the most important factor explaining clinical manifestations.

In typical GDLD patients, bilateral, grayish, elevated round depositions and distinctive severe neovascularization provide enough diagnostic information.[15] However, we and other groups have noticed that there are atypical cases of GDLD that show clinical variability in both age at onset and severity, and in phenotype, even within a family.[8,16]

Family 1 shows clear phenotypic variability within the family. One proband had typical, severe GDLD that required corneal transplantations in both eyes by 31 years of age, whereas his brother had only subepithelial opacification and needed no surgical interventions up to age 39. This brother showed no grayish gelatinous elevation in either eye, and it might have been difficult to diagnose him as having GDLD without a family history. Families 2, 3, and 4 showed phenotypic variability among the families and atypical GDLD.

The cloning of the gene responsible for GDLD enabled us to examine this phenotypic variability on a molecular level. The first question was whether the phenotypic variability was caused by genetic differences within the *TACSTD2* sequence. The phenotypes of GDLD in these patients were quite different; however, the sequence analysis and RFLP results revealed that all patients were homozygous for the Q118X mutation. Therefore, the clinical heterogeneity was clearly not due to allelic or locus heterogeneity. Moreover, the patients showed not only allelic homogeneity, but also shared the same D216E and 204bp-285bp-247bp (D1S2752-D1S2648-D1S220) haplotype, which extends for 400 kb near the *TACSTD2* region. This haplotype is reported to be shared by most typical Japanese GDLD patients,[4,7] indicating that these patients share not only the same disease-causing mutation but also the same chromosomal region, including the same *cis*-acting genetic elements such as the promoter and enhancer. Therefore, we infer that the phenotypic variability among these patients is caused either by *trans*-acting genetic elements or environmental factors.

It is interesting to hypothesize regarding the mechanism of amyloid deposition on the cornea. Corneal amyloidoses occur not only in inherited corneal dystrophies but also as the result of secondary changes after nonspecific chronic disorders and injuries. In these cases, it is usually unilateral, but sometimes it resembles closely the GDLD phenotype. These cases indicate that a genetic factor, such as a *TACSTD2* mutation, is not a prerequisite condition for severe corneal amyloidoses. On the other hand, the amyloid in GDLD has been found to react immunohistochemically with human lactoferrin antibodies and lactoferrin may play a role in amyloid depositions in the cornea.[17,18] The importance of lactoferrin might indicate that several steps may be responsible for amyloid depositions in GDLD, and the malfunctions of *TACSTD2* alone are not enough to account for severe corneal amyloidoses in GDLD. The complex mechanism of amyloid deposition might be one cause of the phenotypic variability presented here. Investigations of factors other than *TACSTD2* malfunctions will lead to better understanding of the mechanism of amyloidoses and more effective therapy without surgical intervention.

We have also reported four other disease-causing mutations in *TACSTD2* (632delA, Q207X, S170X, L186P),[4,19] but we encountered only one homozygous family with each mutation so we could not determine phenotype–genotype correlations among these mutations. However, our impression was that all of those patients had typical GDLD and those among them with the most severe disease possessed the Q207X mutation (data not shown), which translates into a product with a longer carboxyl terminus than the Q118X mutation product. Following those investigations, we now believe that phenotype–genotype correlations may not be involved. The lack of a clear phenotype–genotype correla-

tion indicates that a genetic factor is not an important key to the severity of GDLD, although the dysfunction of *TACSTD2* is necessary for the onset of GDLD. This hypothesis is also supported by the variabilities in the cases we presented.

The phenotypic variability presented here is also important in the diagnosis of GDLD. In families 2, 3, and 4, the patients were not diagnosed with GDLD on the basis of clinical features and examinations. In the family 3 patient, the palisades of Vogt were distinguished and apparent lipid deposition was observed; therefore, we diagnosed him as having typical spheroidal corneal dystrophy. In the patient of family 2, neovascularization, recognized as an important clinical feature of GDLD, was not observed. In such cases, without any significant family history of GDLD, it may be difficult to diagnose the presenting symptoms as GDLD. Thus, these patients were misdiagnosed as having either spheroidal corneal degeneration or macular corneal dystrophy.

On the other hand, late fluorescent staining was observed in all of the patients presented here. That it is an important clinical feature in GDLD diagnosis, and this phenomenon is well explained by the high epithelial permeability observed in GDLD corneas.[20,21] In these atypical cases, the genetic diagnosis presented here in addition to positive late staining of the corneal epithelium is quite useful for diagnosing GDLD, in spite of the possible presence of locus heterogeneity.[22]

Acknowledgments. Drs. Jarema Malicki and Koji Nishiguchi provided many helpful comments on the previous versions of this manuscript. This study was supported by Grants-in-Aid from the Ministry of Education, Culture, Sports, Science and Technology (to M.T.) and by Grants-in-Aid from the Ministry of Health, Labour and Welfare (to M. T.).

References

1. Nakaizumi G. A rare case of corneal dystrophy. Acta Soc Ophthalmol Jpn 1914;18:949–950.
2. Weber FL, Babel J. Gelatinous drop-like dystrophy. A form of primary corneal amyloidosis. Arch Ophthalmol 1980;98:144–148.
3. Tsujikawa M, Kurahashi H, Tanaka T, et al. Homozygosity mapping of a gene responsible for gelatinous drop-like corneal dystrophy to chromosome 1p. Am J Hum Genet 1998;63:1073–1077.
4. Tsujikawa M, Kurahashi H, Tanaka T, et al. Identification of the gene responsible for gelatinous drop-like corneal dystrophy. Nat Genet 1999;21:420–423.
5. Fujiki K, Nakayasu K, Kanai A. Corneal dystrophies in Japan. J Hum Genet 2001;46:431–435.
6. Yamamoto S, Okada M, Tsujikawa M, et al. The spectrum of beta ig-h3 gene mutations in Japanese patients with corneal dystrophy. Cornea 2000;19:S21–23.
7. Tsujikawa M, Tsujikawa K, Maeda N, et al. Rapid detection of M1S1 mutations by the protein truncation test. Invest Ophthalmol Vis Sci 2000;41:2466–2468.
8. Ide T, Nishida K, Maeda N, et al. A spectrum of clinical manifestations of gelatinous drop-like corneal dystrophy in Japan. Am J Ophthalmol 2004;137:1081–1084.
9. Grimberg J, Nawoschik S, Belluscio L, McKee R, Turck A, Eisenberg A. A simple and efficient non-organic procedure for the isolation of genomic DNA from blood. Nucleic Acids Res 1989; 17:8390.
10. Munier FL, Korvatska E, Djemai A, et al. Kerato-epithelin mutations in four 5q31-linked corneal dystrophies. Nat Genet 1997;15: 247–251.
11. Korvatska E, Munier FL, Djemai A, et al. Mutation hot spots in 5q31-linked corneal dystrophies. Am J Hum Genet 1998;62:320–324.
12. Mashima Y, Imamura Y, Konishi M, et al. Homogeneity of kerato-epithelin codon 124 mutations in Japanese patients with either of two types of corneal stromal dystrophy. Am J Hum Genet 1997; 61:1448–1450.
13. Mashima Y, Yamamoto S, Inoue Y, et al. Association of autosomal dominantly inherited corneal dystrophies with BIGH3 gene mutations in Japan. Am J Ophthalmol 2000;130:516–517.
14. Konishi M, Yamada M, Nakamura Y, et al. Varied appearance of cornea of patients with corneal dystrophy associated with R124H Mutation in the BIGH3 gene. Cornea 1999;18:424–429
15. Smolin G. Corneal dystrophies and degenerations. In: Smolin G, Thoft R, editors. Cornea, 3d ed. Boston: Little, Brown; 1994. p. 499–533.
16. Yoshida S, Kumano Y, Numa S, et al. Two brothers with gelatinous drop-like dystrophy at different stage of the disease; role of mutation analysis. Am J Ophthalmol 2002;13:830–832.
17. Klintworth GK, Valnickova Z, Kielar RA, Baratz KH, Campbell RJ, Enghild JJ. Familial subepithelial corneal amyloidosis—a lactoferrin-related amyloidosis. Invest Ophthalmol Vis Sci 1997; 38:2756–2763.
18. Araki-Sasaki K, Ando Y, Nakamura M, et al. Lactoferrin Glu-561Asp facilitates secondary amyloidosis in the cornea. Br J Ophthalmol 2005;89:684–688.
19. Taniguchi Y, Tsujikawa M, Hibino S, et al. A novel missense mutation in a Japanese patient with gelatinous droplike corneal dystrophy. Am J Ophthalmol 2005;139:186–188.
20. Kinoshita S, Nishida K, Dota A, et al. Epithelial barrier function and ultrastructure of gelatinous drop-like corneal dystrophy. Cornea 2000;19:551–555.
21. Kinoshita S, Adachi W, Sotozono C, et al. Characteristics of the human ocular surface epithelium. Prog Retin Eye Res 2001;20: 639–673.
22. Klintworth GK, Sommer JR, Obrian G, et al. Familial subepithelial corneal amyloidosis (gelatinous drop-like corneal dystrophy): exclusion of linkage to lactoferrin gene. Mol Vis 1998;4:31.